Resistance of Clay Brick Masonry Façades to Wind-Driven Rain

Repointing of Eroded Mortar Joints

Kahangi, Mohammad

2021

Document Version:
Publisher's PDF, also known as Version of record

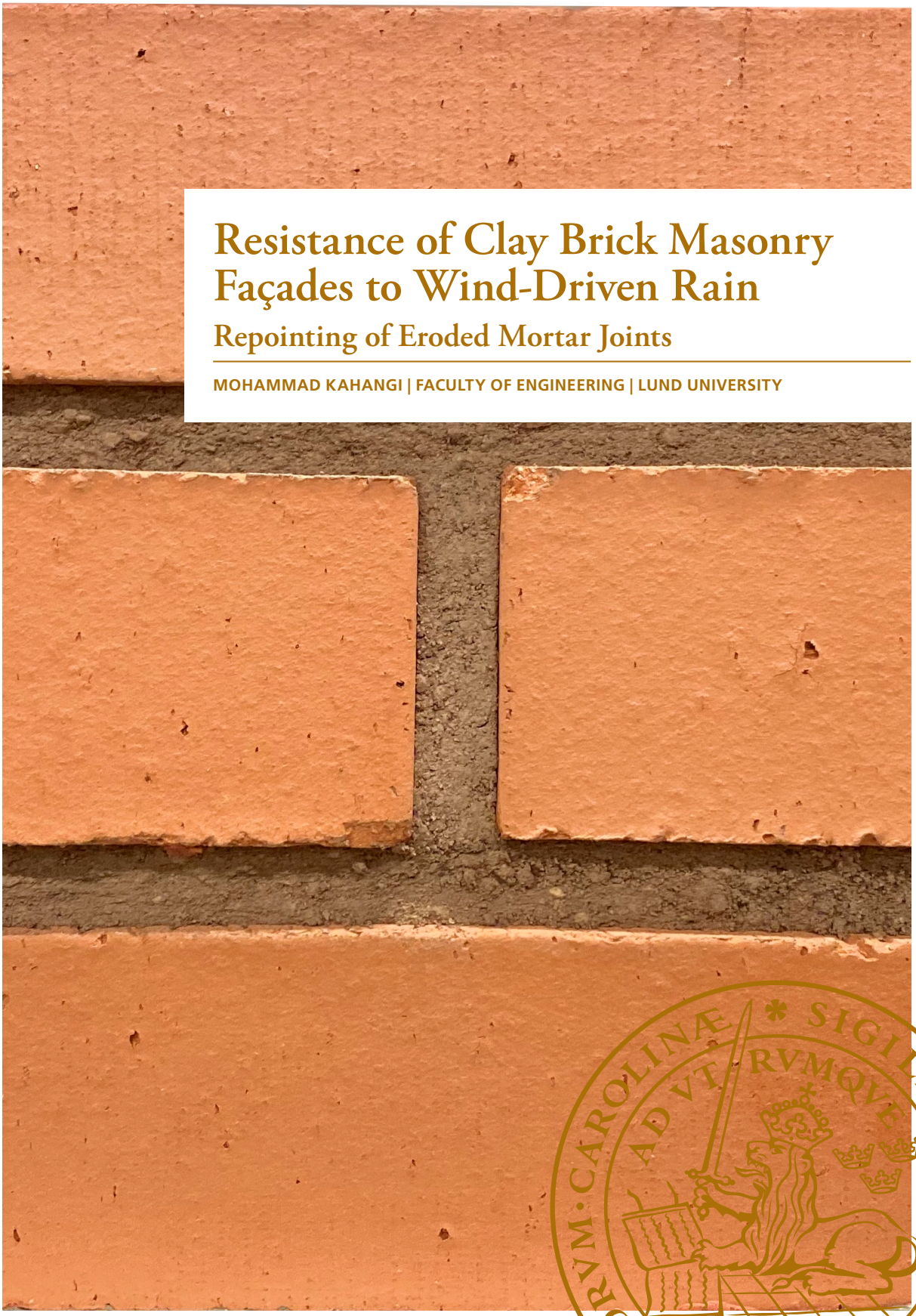

Resistance of Clay Brick Masonry Façades to Wind-Driven Rain

Repointing of Eroded Mortar Joints

MOHAMMAD KAHANGI | FACULTY OF ENGINEERING | LUND UNIVERSITY

Resistance of Clay Brick Masonry Façades to Wind-Driven Rain

Repointing of Eroded Mortar Joints

by Mohammad Kahangi

LUND UNIVERSITY

LICENTIATE THESIS

Faculty opponent
Dr. Carl-Magnus Capener
RISE – Research Institute of Sweden

To be defended, by due permission of the Faculty of Engineering, Lund University, Sweden, in the lecture hall A:C, A-Huset, Sölvegatan 24, Lund, on Friday, the 1st of October 2021 at 13:00.

Organization	Document name
LUND UNIVERSITY Department of Building and Environmental Technology Division of Structural Engineering Box 118, SE–221 00 LUND, Sweden	**Licentiate Thesis** Date of disputation **2021-10-01**
Author(s) **Mohammad Kahangi**	Sponsoring organization

Title and subtitle

Resistance of clay brick masonry façades to wind-driven rain: Repointing of eroded mortar joints

Abstract

Clay brick masonry façades are commonly used due to their high-performance durability. However, exposure to climate agents such as wind-driven rain (WDR), freeze-thaw cycles, and wind abrasion cause deterioration of masonry façades over time. WDR as a significant source of moisture may contribute to the erosion of mortar joints and lead to increased moisture content and risk of water penetration. Accordingly, a maintenance technique, repointing of eroded mortar joints, is recommended as a measure to mitigate moisture/water penetration related to WDR. Repointing is a labor-intensive and costly measure, and there are today no established criteria to determine when repointing is necessary. As such, to enable rational decision-making in maintenance, there is a need for a systematic approach to assessing the need for repointing.

Water penetration in masonry exposed to WDR is dependent on a wide range of parameters such as rain intensity, wind velocity, building geometry, the presence of cracks, the profile of mortar joints, the type and quality of masonry units, the compatibility of units and mortar, and the workmanship. There are several experimental methods available through standards and research studies aiming to study water penetration in masonry. Nevertheless, the test conditions, including water spray rate and differential air pressure, of those methods are rather extreme and not representative of actual conditions.

In this regard, a new test setup has been developed to study water absorption and penetration in masonry. The key feature is to enable uniform water spray exposure at considerably lower water application rates than in existing standards while continuously recording both the amount of absorbed and penetrated water. Further, the test setup was equipped with a digital camera to record visible dampness, enabling the damp area on the backside of the specimen to be monitored over time. The test setup was used in two experimental campaigns to study the interaction of clay brick masonry and WDR, providing a fundamental basis for developing a framework for rational repointing of clay brick masonry façades.

In the first experimental campaign, two series of clay brick masonry specimens were prepared, with two different types of bricks and three different mortar joint profiles. As a representative of eroded mortar joints, specimens with the raked joint profiles were prepared to study how eroded mortar joints might affect WDR related water absorption and penetration. The tests were conducted at zero differential air pressure, at water spray rates varying between 1.7 and 3.8 l/m^2/h. In the second experimental campaign, the water spray rate was increased to around 6.3 l/m^2/h; yet no air pressure was applied. Further, compared to the first campaign, three different types of bricks with different water absorption properties were considered.

The obtained results indicate that water absorption and penetration are highly dependent on the water spray rate and water absorption properties of bricks, whereas the effect of mortar joint profile on water absorption and penetration is negligible. It should be mentioned that no considerable amount of water penetration in the first campaign was recorded; hence, only the results regarding water absorption and damp patches are presented for the first campaign. The newly developed test setup might facilitate verification of moisture simulations and provide a basis for rational decision-making concerning clay brick masonry design and maintenance.

Keywords: **clay brick masonry façade, wind-driven rain, water absorption, water penetration, damp patches**

Classification system and/or index terms (if any)

Supplementary bibliographical information		Language **English**
ISSN and key title **0349-4969**		ISBN **978-91-87993-20-6**
Recipient's notes	Number of pages **63**	Price
	Security classification	

Signature  Date 2021-08-23

Resistance of Clay Brick Masonry Façades to Wind-Driven Rain

Repointing of Eroded Mortar Joints

by Mohammad Kahangi

LUND
UNIVERSITY

Front and back cover photos by Mohammad Kahangi

Faculty of Engineering
Department of Building & Environmental Technology
Division of Structural Engineering

Report: TVBK-1055
ISBN: 978-91-87993-20-6
ISSN: 0349-4969
ISRN: LUTVDG/TVBK-21/1055 (63)

Printed in Sweden by Media-Tryck, Lund University
Lund 2021

Table of Contents

Preface

The presented thesis is submitted for the licentiate degree at Lund University. The author conducted the research described herein under the supervision of Dr. Miklós Molnár at the Division of Structural Engineering, Lund University, between September 2019 and September 2021.

I would like to express my gratitude to my main supervisor, Dr. Miklós Molnár, and assistant supervisor, Tekn. Lic. Tomas Gustavsson, who drew the outline of the project. Constructive supervision, patience, and support of Miklós have helped me to accomplish my study goals. Thank you so much for all your encouragement, sharing knowledge, and always providing helpful feedback. Further, I would like to thank my co-supervisor, Dr. Jonas Niklewski, a caring friend and patient colleague with exceptional input and golden hands in programming and image analysis. I would like to thank my assistant supervisors, Tekn. Lic. Tomas Gustavsson, Dr. Eva Frühwald Hansson, and Dr. Ivar Björnsson, for their excellent guidance and support during this project. I am also grateful for the support given by Per-Olof Rosenkvist, without whose cooperation I would not have been able to conduct the experimental part of the project. I also wish to thank all the reference group members.

The project would not have been possible to be carried out without the financial support of the Development Fund of the Swedish Construction Industry (SBUF) and the Masonry and Render Construction Association (TMPB).

To my other colleagues, Amro, Iman, and Oskar, at the Division of Structural Engineering: I would like to thank you for your outstanding cooperation as well. It was always helpful to bat ideas about my research around with you. I also benefitted from debating issues with my friends and family.

Mohammad Kahangi

List of Publications

I. **Shahreza, S.**, Molnár, M., Niklewski, J., Björnsson, I., & Gustavsson, T. (2020). **Making decision on repointing of clay brick facades on the basis of moisture content and water absorption tests results–a review of assessment methods.** *In the proceedings of the 17th International Brick/Block Masonry Conference (17th IB2MaC 2020), Kraków, Poland, (pp. 617-623). CRC Press/Balkema*.

II. **Shahreza, S. K.**, Niklewski, J., & Molnár, M. (2021). **Experimental investigation of water absorption and penetration in clay brick masonry under simulated uniform water spray exposure**, *Journal of Building Engineering, vol. 43, p. 102583, 2021, doi*: https://doi.org/10.1016/j.jobe.2021.102583.

III. **Shahreza, S.**, Molnár, M., & Niklewski, J. (2021). **Water absorption and penetration in clay brick masonry exposed to uniform water spray**. *In the proceedings of the 14th Canadian Masonry Symposium (14th CMS), Montreal, Quebec, Canada, 16–20 May 2021*.

Summary

Clay brick masonry is a building material commonly used in façades because of its high durability and a reduced need for costly maintenance. While being a comparatively slow process, brick masonry façades deteriorate over time due to climate agents such as cyclic freezing-thawing and wind-driven rain (WDR), making continual monitoring and frequent maintenance of masonry façades necessary. WDR is a significant source of moisture and a leading cause of mortar joint erosion in Nordic countries. High levels of moisture and water penetration resulting from WDR can cause corrosion of reinforcement, promote microbiological growth, and compromise indoor air quality. Accordingly, maintenance techniques such as repointing of eroded joints can be used to control moisture content and water penetration and to protect moisture-sensitive parts of the building envelope.

There are several benefits to repointing. Primarily, it is expected that repointing can reduce the risk of issues stemming from the increased penetration of WDR caused by eroded mortar joints. Further, repointing may lead to improving the aesthetics and maintain the integrity of the façade. However, there are also several risks related to improper repointing, such as the risk of damaging the bricks or the existing mortar. In addition, repointing is both a laborious and expensive measure.

Repointing should not be carried out in situations when it is not required. Today, repointing is generally carried out at regular intervals ranging between 40-50 years, even if not necessary. In order to improve current practice, more well-established criteria to assess the actual need for repointing are required. In order to do so, the resistance of masonry façades to frequent WDR events encountered in Nordic countries should be understood. Secondly, the effects of erosion and repointing of mortar joints need to be established. This information can ultimately be used in a cost-benefit analysis to enable rational decisions on the maintenance of clay brick façades.

There are many parameters affecting moisture content and water penetration of masonry façades. The first group of parameters consists of characteristics of rain and wind, including rain intensity, raindrop size, wind velocity, and wind direction. The second group is related to the characteristics of the masonry, including material properties (absorption properties of brick and mortar), joint profile, mortar water content, and joint thickness. However, masonry walls with the same prescribed characteristics may differ widely in performance due to workmanship during construction.

The primary goal of the studies presented in this thesis is to investigate the resistance of clay brick masonry façades exposed to realistic WDR events, providing basic knowledge to make rational decisions on maintenance techniques, with a focus on repointing. Experimental campaigns were designed to explore the masonry-water interaction during exposure to WDR. The test parameters include water spray rate,

water absorption properties of bricks, and mortar joint profiles. A newly developed test setup capable of producing a wide range of WDR intensities with a uniform water spray is designed. The test conditions are adapted to be representative of WDR events encountered on the west coast of Sweden.

The results indicate that mortar joint erosion may not affect to a significant degree water absorption and penetration in masonry exposed to WDR. Furthermore, the benefit gained from the water absorption capacity of clay brick masonry to buffer and thus postpone water penetration is of great importance. Considering frequent WDR events where the average WDR intensity usually varies between 1–2 mm/h, and wind speed is less than 5 m/s, equivalent to 20 Pa pressure difference, clay brick masonry façades are capable of absorbing most of the raindrops prior to water penetration.

There are several techniques available that may reveal the real need for repointing or postpone costly maintenance techniques. Washing the masonry façade gently with water and cleaning microbiological growth might reveal the depth of erosion and cracks. Washing might also reduce the fixation of water to clay brick façades. Further, hairline cracks that are not deep through the masonry wall can be treated by so-called surface grouting, expected to reduce water absorption during WDR events.

Based on the previous observations and analyses of climate data, usually, one or two faces of a building are exposed to more wind-driven rain than the other faces. Therefore, partial repointing can be considered as an alternative, reducing the maintenance costs compared to full repointing.

1 Introduction

1.1 Background

Clay brick masonry is one of the most common building materials used in external walls and building façades, with a history spanning many thousands of years and applications throughout the world. Its longevity and ubiquitous use provide some insight into clay brick masonry's excellent durability and long-term performance. In addition to the impacts of material properties and workmanship on the durability of masonry, performance degradation due to exposure to climate agents such as wind-driven rain (WDR) and freeze-thaw cycles is notable. WDR is a significant source of moisture ingress and a leading cause of the erosion of mortar joints, further associated with elevated moisture accumulation and increased risk of water penetration.

The co-occurrence of wind and rain giving rise to an oblique driving rain vector, that together with the presence of deficiencies like cracks, voids, and pores, may result in water penetration. Water penetration through façades depends on several parameters categorized into two groups. The first group is related to the WDR deposition rate on building façades, including rain intensity, raindrop size, wind velocity and its direction, building geometry and its height, and topography. The second group of parameters is related to the façade characteristics such as the presence of cracks, the profile of mortar joints, the type and quality of masonry units, the type of mortar and its consistency, the compatibility of units and mortar, joint thickness, and the workmanship.

In addition to the impact of WDR on the aesthetics of masonry façades, high levels of moisture and water penetration resulting from WDR can cause corrosion of reinforcement and promote microbiological growth, leading to the physical deterioration of the envelope and of the quality of indoor air through the emission of mycotoxins and organic volatiles [1]. Performing maintenance is thus necessary to ensure the long-term performance of the structure, reduce the speed of deterioration, and guarantee the comfort of its users.

A typical maintenance technique to mitigate moisture/water penetration related to WDR in brick masonry façade is repointing, recommended being carried out after 40–50 years of the façade erection. Repointing is the process of raking out the eroded/cracked mortar joints to a certain depth and replacing it with new mortar.

The motivation for repointing is often brought up when eroded mortar joints, cracks in the mortar, gaps between the mortar and masonry unit, damp surfaces on the masonry, and water infiltration on the interior walls are observed [2].

On the one hand, repointing of the eroded joints may improve the resistance of the masonry façade to WDR and keep the integrity of the masonry. On the other hand, repointing only to improve the aesthetics of the façade may also be unsuitable owing to the high costs and relatively complex procedures for carrying out repointing. Additionally, repointing can lead to premature deterioration of the mortar and the masonry unit, such as erosion of the edges of soft masonry units and discoloration of the masonry units if it is not done properly. Hence, there is a need to shed light on how the erosion of mortar joints influences water uptake and penetration exposed to WDR, providing a basis for making rational decisions on repointing. In order to do so, there is a need to understand the basic interaction of clay brick masonry exposed to realistic WDR intensities.

Various test setups have been proposed in different standards and research studies to explore water penetration in masonry [3-10], yet the applied water spray and air pressure rates represent rather extreme WDR conditions [3-9, 11-14]. Hence, several authors have pointed out the need to develop a simple test setup able to operate at considerably lower water application rates [6, 9, 15-18]. Accordingly, several studies were carried out with adjusting test conditions, including differential air pressure [5, 12, 19, 20] and water spray rate [18, 21, 22]. Therefore, to better understand brick masonry resistance to WDR, there is a need to adapt the test parameters of the available standards.

1.2 Objectives

The primary objective of the presented thesis is to provide an adequate understanding of the clay brick masonry response exposed to more realistic and frequently encountered WDR events. It is expected that the outcomes lead to solid and scientific knowledge to be used in the context of assessing repointing needs. In doing so, water absorption and penetration in masonry as a function of brick and mortar material properties were studied. Additionally, the effect of mortar joint erosion on water absorption and penetration in masonry was investigated.

1.3 Limitations

The experimental investigation presented here is limited to studying the exposure of small-scale brick masonry specimens to uniform water spray, whereas a masonry

façade includes windows, joints, and other connections that are expected to be more vulnerable to WDR exposure. Moreover, masonry façades are exposed to different rain and wind events in the long term, resulting in high moisture levels, erosion of mortar joints, and leakage, whereas exposing masonry façades to real WDR events in the laboratory is not achievable.

Additionally, specimens tested in this study were built without any known cracks and deficiencies, whereas many existing masonry façades contain cracks either on bricks or mortar joints. Further, because of the difficulty of preparing specimens with eroded mortar joints, specimens with a raked joint profile were chosen as a representative of eroded joints. However, erosion of mortar joints happens after long-term exposure to WDR, wind abrasion, and freezing-thawing, leading to higher porosity and change of mortar properties.

1.4 Outline of the thesis

The thesis is divided into seven chapters. Chapter 1 introduces the background, objectives of the research, and limitations of the current work. At the beginning of Chapter 2, repointing as a maintenance technique to diminish WDR related issues is introduced, and motivations to make a decision on repointing are discussed. Subsequently, two categories of wind-driven rain studies in relation to building research are discussed. Eventually, as moisture is one of the leading causes of the damage on building façades, moisture transport mechanisms within porous media like masonry are described. Chapter 3 presents a newly developed test setup used to study the exposure of masonry to WDR. Relevant properties of materials and preparation of masonry specimens are described. Chapter 4 focuses on the experimental results, including water absorption and penetration in clay brick masonry. A summary of the appended papers is provided in Chapter 5. The thesis is concluded with a conclusion in Chapter 6, and finally, suggestions for future research are proposed in Chapter 7.

2 Theoretical Framework

In this chapter, repointing as a maintenance technique that is supposed to diminish WDR related problems is introduced, and motivations to make a decision on repointing are discussed. Subsequently, two categories of WDR studies concerning building research are discussed. Different methods to quantify WDR deposition are further introduced, and a well-known and frequently used model, the ISO Standard, to quantify WDR deposition on building façades is presented in detail. The presented model is then applied to study WDR deposition for different locations in Sweden. The obtained results can provide a rational basis for designing the experimental studies and being applied in the test setups. Eventually, since moisture is one of the leading causes of damage on building façades, moisture transport mechanisms within porous media like masonry are presented.

2.1 Repointing

Maintenance due to inevitable deterioration caused by climate actions is needed to ensure the durability performance of a clay brick masonry façade during its expected service lifespan, which often exceeds a hundred years. Climate agents relevant to Nordic countries, including WDR and freeze-thaw cycles, are a significant cause of spalling, delamination, or cracking of bricks and the erosion and cracking of mortar joints. Prior to performing any maintenance, a preliminary assessment including visual inspection with reviewing existing documentation is highly recommended to determine the source and the severity of probable existing damages/problems. Besides, performing tests (non-destructive or destructive) might add valuable information to the state assessment of the façade. Rational decisions can then be made based on the analysis of the information at hand through a cost-benefit analysis. Several recommendations on practical tools to assess the state of the façade and relevant maintenance techniques are reported in Paper I.

One maintenance technique often carried out nowadays in order to tackle problems raised by eroded/cracked mortar joints is repointing. Repointing is the process of raking out existing mortar joints to a certain depth, usually 25 mm, and then replacing them with new mortar that should be compatible with the existing mortar and bricks. Figure 1 illustrates a clay brick masonry façade before, during, and after repointing.

Figure 1. A clay brick masonry façade, before and after repointing a) the initial state where mortar joints were eroded; b) mortar joints were raked out up to the depth of 25 mm; c) new mortar was pointed.

A common argument for repointing is that the erosion of mortar joints facilitates water uptake in façades exposed to WDR [23]. Further, erosion of mortar joints is regarded as unfavorable from an aesthetic point of view, at least in the Nordic countries, since it creates, seen superficially, the impression of building damages. According to the present practice in the Nordic countries, repointing shall be carried out as part of a regular maintenance scheme, after 40-50 years from erection or when limited façade parts with more or less eroded mortar joints are observed [24, 25]. Normally, no further investigations (e.g., concerning factual water up-take) nor alternative measures (e.g., partial repointing of eroded parts) are considered. In light of the presented practices, it can be objected that decision concerning the repointing of clay brick façades is usually not based entirely on rational grounds.

Although repointing is expected to reduce water ingress from WDR [26], repointing to improve only the aesthetics of the façade or, in the case of minor signs of erosion, regardless of its laborious task, may imply unnecessary costs [27, 28]. Since natural sands were used in the mortar mix of many old masonry façades, in the case of repointing, sand made from crushed stones is normally used because of the limited source of natural sands; under this circumstance, repointing will not improve aesthetics. Improper selection and application of repointing mortars can further result in permanent damage to older masonry walls [29, 30]. Specific problems include incompatibility between the new mortar and existing mortar [31] or between the new mortar and bricks (i.e., the weak bond between new mortar and existing bricks) [32, 33], as well as poor workmanship. Thus, in the case of unnecessary repointing, there is a higher risk of aesthetic matters and durability problems in the form of frost damage and spalling of the façade [34]. Figure 2 exemplifies the

adverse effects of selecting improper mortar and poor workmanship during repointing.

Accordingly, there is a need for a systematic approach to decide when repointing is needed and how it should be carried out. Recommended steps to reach a rational decision on repointing are further discussed in Paper I.

Figure 2. An example of adverse effects of selecting unsuitable mortar and shoddy workmanship on repointing

Qualitative and quantitative criteria concerning the need for repointing have been proposed by several researchers, e.g. [24, 26, 35-37], recommending repointing when a) the surface of the mortar joints contains hairline cracks, b) eroded mortar joints to a certain depth [a quarter of an inch, i.e., 6.4 mm] have been observed, c) crack widths larger than 2 mm have been measured, d) the rate of water absorption is more than 4.5 $l/m^2/h$ or e) presence of voids has been detected. According to the proposed criteria, it should be investigated to what extent high moisture content and water absorption/penetration are related to the outer part of the mortar joints and whether repointing can make a difference in reducing water absorption/penetration [29, 32]. It should be noted that only 25 mm of the outer part of the cracked/eroded mortar joints or 2.5 times of the mortar joint thickness is normally raked out and replaced with a new mortar in repointing. In this context, the relation between the depth of erosion of the mortar joints and the possible increase in water absorption and penetration from WDR should be examined. Furthermore, the rationality of some of the proposed criteria can be questioned and needs to be investigated, e.g., concerning acceptable crack width, since it has been shown that water ingress in cementitious materials increases exponentially when the crack width exceeds 0.2 mm [38, 39].

2.2 Wind-driven rain

WDR is one of the most important moisture sources affecting the performance of building façades and resulting in the erosion of mortar joints. Therefore, the study of WDR in order to quantify WDR intensity on building façades is essential for hygrothermal and durability analyses. Further, a framework is required to understand frequent WDR events in regions with moderate WDR events, which then can be a rational basis for test conditions in experimental studies.

2.2.1 Measurements and calculations

Generally, studies of WDR consist of two categories; i) the first one mainly deals with quantifying WDR deposition on building façades, and ii) the second category studies the response of buildings to WDR impingement and its effect on building façades. In order to assess the hygrothermal performance of a building envelope, the appropriate estimation of the amount of rainwater striking the building's façade, the first category of WDR studies, is required.

Three different methods, namely, a) experimental, b) semi-empirical, and c) numerical, are used to quantify WDR deposition on building façades. The WDR intensity depends on several factors such as rain intensity, raindrop size, wind speed and its direction, building geometry, and topography.

In experimental methods, rain gauges are used to measure WDR on building façades, and since there is no standardized rain gauge [40], there can be a significant difference in the measurements. Although experimental measurements are still needed to validate semi-empirical and numerical models [40, 41], they are time-consuming and costly, as they should be continued for more extended periods.

Therefore, semi-empirical relationships were established to obtain WDR exposure of building façades based on standard weather data, including wind speed, wind direction, and horizontal rainfall. In order to improve the accuracy of semi-empirical equations, two main modifications are taken into account in different models; a) factors such as building geometry, local topography, and presence of obstruction are considered; b) hourly rainfall and wind speed data are normally used to estimate WDR deposition. Nevertheless, semi-empirical methods are generally accurate only for stand-alone buildings in simple configurations or for preliminary analyses. These methods will not give accurate results in cases where complex flows around buildings due to the influence of the surrounding buildings are observed [40].

Because of the shortcomings in the measurement of WDR in both experimental and semi-empirical methods, numerical methods based on computational fluid dynamics (CFD) can be used to account for building geometry by simulating wind-flow

patterns and trajectories of raindrops. However, the method is far complicated, computationally expensive, and time-consuming.

The second category of WDR studies investigates phenomena such as splashing, bouncing, spreading, and absorption of raindrops, water film and its absorption, moisture accumulation and water content in walls, rain penetration, and runoff [42]. In this regard, Erkal et al. [43] and Abuku et al. [44] have studied splashing, bouncing, spreading, and absorption of raindrops when hitting masonry façades. Further, several studies on the rain absorption and the rainwater runoff, which are responsible for water leakage in building façades and the appearance of surface soiling patterns on façades, have been conducted by Carmeliet and Blocken [45], Robinson and Baker [46], and Newman et al. [47].

By considering the same size for all raindrops and a uniform and steady wind, the general equation for WDR intensity, i.e., water drops passing through an imaginary vertical plane, is expressed as [48, 49]:

$$R_{wdr} = R_h \cdot \frac{U}{V_t} \quad (1)$$

where R_h is the horizontal rain intensity (mm/h), U is the wind speed (m/s), and V_t is the terminal velocity of raindrops (m/s).

In Eq. (1), wind direction is considered perpendicular to the vertical surface, and the assumption is that there is no deflection of wind and raindrops by the vertical surface. Lacy [49] proposed a similar relationship (Eq.(2)) for WDR intensity by considering various results from observations, as presented below:

$$R_{wdr} = 0.222 \cdot U \cdot {R_h}^{0.88} \quad (2)$$

where 0.222 (s/m) is the WDR coefficient.

The model by Lacy [49] considers the WDR coefficient resulting from the adopted empirical relationships. The associated WDR coefficient of 0.222 s/m was derived for free-field conditions (i.e., free driving rain) and corresponds to a raindrop diameter of 1.2 mm, a realistic value for rain events of light to moderate intensity [50].

To determine the WDR coefficient on a building façade more accurately, several parameters, including building geometry and topography, should be considered. Accordingly, the semi-empirical models proposed by Straube and Burnett (SB) [51] and ISO Standard [52], and the numerical model developed by Choi [53] attempt to quantify the WDR coefficient and WDR intensity by taking into account several parameters such as building geometry, position on façade, environment topography, mean wind speed, and wind direction [54].

In order to take into account disturbed wind-flow patterns around the building, which results in a considerable difference between the WDR intensity in free-field conditions and the WDR intensity on a building façade, an adapted WDR coefficient, α, was introduced. Hence, the WDR relationship can be written as follows:

$$R_{wdr} = \alpha \cdot U \cdot {R_h}^{0.88} \cdot \cos\theta \quad (3)$$

where α is the WDR coefficient (s/m), and θ is the angle between the wind direction and the normal to the façade.

The ISO Standard of 2009 [52] is mainly established according to the BS 8104 [55] code, based on a long series of WDR measurements within the UK. It should be noted that the model primarily applies to climates similar to the UK. Four main parameters are used in the ISO model to convert the amount of rain that would be collected by a free-standing rain gauge in a flat open field into the amount of rain that would impact a façade. Thus, the WDR coefficient in the ISO model is calculated as follows.

$$\alpha = \frac{2}{9} \cdot C_R \cdot C_T \cdot O \cdot W \quad (4)$$

where C_R is the terrain roughness coefficient, C_T is the topography coefficient, O is the obstruction factor, and W is the wall factor.

The roughness coefficient, C_R, takes into account the variability of mean wind velocity at the site due to the height above the ground and the roughness of the terrain. The ISO model defines four different terrain categories and their relevant parameters to determine the roughness coefficient, C_R at height z, which is calculated as follows.

$$\mathrm{C_R(z)} = \mathrm{K_R} \cdot \ln\left(\frac{\mathrm{z}}{\mathrm{z_0}}\right) \text{ for } \mathrm{z} \geq \mathrm{z_{min}} \quad (5)$$

$$\mathrm{C_R(z)} = \mathrm{C_R(z_{min})} \text{ for } \mathrm{z} < \mathrm{z_{min}} \quad (6)$$

where z is the height above ground [m]; K_R is the terrain factor [-]; z_0 is the roughness length [m], and z_{min} is the minimum height [m].

In order to account for the increase in mean wind speed over hills and escarpments, the topography coefficient, C_T is introduced, depending on the upwind slope. The obstruction factor, O, takes into account the horizontal distance between the exposed wall and the nearest obstacle, which is at least as high as the wall. Thus, depending on the distance to the nearest obstacle, the obstruction factor varies in the range of 0.2 and 1.0. The wall factor, W, considers wall types, overhangs, and the orientation of bricks affecting the amount of rain incident on a wall. Hence, the wall factor is

considered to be between 0.2 and 0.5 and varies along with the height of the wall. Despite many WDR measurements indicating that the WDR intensity increases from the middle of the façade to the sides [40], the ISO Standard assumes the same wall factor across the width of the wall.

2.2.2 WDR intensities at four sites in Sweden

In this study, ISO Standard [52], one of the most frequently used models, has been used to provide general information about WDR intensity in Sweden, which can be used as a rational basis for test conditions. In doing so, four locations, namely, Malmö, Gothenburg, Uppsala, and Hörby, located in different regions of Sweden, are studied to analyze WDR intensities. It should be mentioned that the hourly rain intensities and wind velocities in Malmö, Gothenburg, Uppsala, and Hörby for the period 1995 – 2020 are used. The climate data is taken from the Swedish Meteorological Hydrological Institute (SMHI) [56].

To have a better picture of WDR intensities that impacted a building façade during 1995 – 2020, a low-rise building with a 15-m height is considered. It is assumed that the wind direction is perpendicular to the façade ($\theta = 0°$) and the building neighbors to farmlands, thus belonging to terrain category II, according to the ISO model. Values of K_R, z_0, and z_{min} as a function of the terrain category are given in the ISO model, in which $K_R = 0.19$, $z_0 = 0.05$ m, and $z_{min} = 4$ m for terrain category II. Thus, the roughness coefficient C_R is equal to 1.084. Additionally, the building is considered to be located in a flat terrain without any obstruction in its surrounding. Hence, the topography coefficient, C_T, and obstruction factor, O, are equal to one. The wall factor, W, for a multi-story building without any overhang and protection, is equal to 0.5 for the upper part of the façade. Therefore, for the considered building, the WDR coefficient, α, is equal to 0.12 s/m.

Figure 3 illustrates the cumulative time-frequency distribution of WDR intensities for the particular building located in Malmö, Gothenburg, Uppsala, and Hörby for the time period between 1995 and 2020. As can be seen, the majority of WDR events occurred with an intensity of less than 1 mm/h. Nevertheless, the highest WDR intensity varies between 8.5 and 36 mm/h for the studied locations during 1995 – 2020.

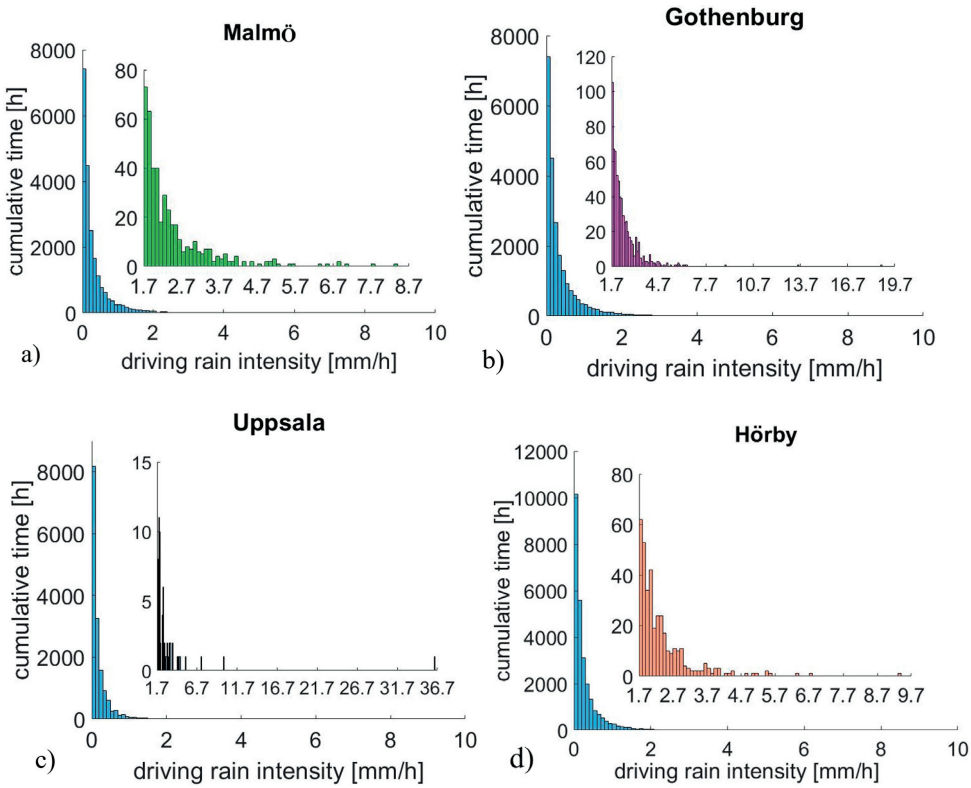

Figure 3. Driving rain intensities from 1995 to 2020 for the considered building located in a) Malmö, b) Gothenburg, c) Uppsala, and d) Hörby

Furthermore, the duration of each WDR event with an intensity of at least 0.1 mm/h for each location is shown in Figure 4. The figure indicates that the majority of WDR events lasted around 1 h to 4 h, though the maximum duration of WDR events was between 23 h and 33 h for the studied locations.

Additionally, the average hourly wind speed at 10 m above ground during WDR spells with an intensity of at least 0.1 mm/h was between 2.7 m/s and 4.2 m/s for the studied locations. Therefore, the mentioned wind speeds impose a pressure difference of less than 10 Pa across the building envelope. Moreover, during the period of 1995 to 2020, the maximum registered wind speed during rainfall events for the studied locations varied between 9.2 m/s and 18.5 m/s, corresponding to an air pressure difference of around 55 Pa – 220 Pa.

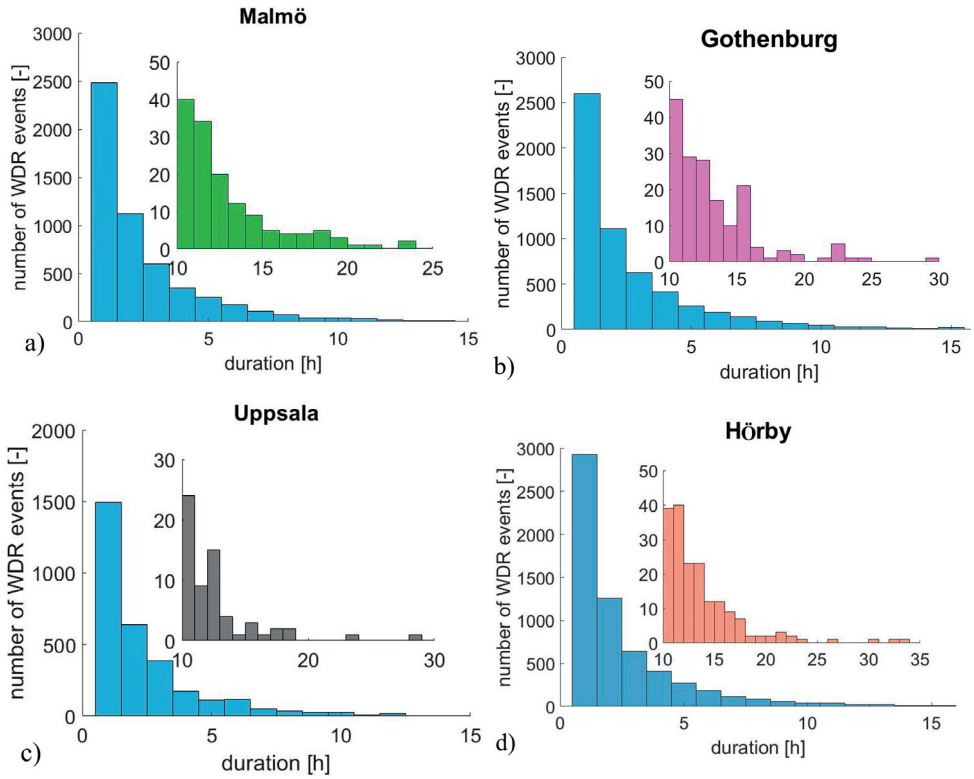

Figure 4. Number and duration of WDR events from 1995 to 2020 for the considered building located in a) Malmö, b) Gothenburg, c) Uppsala, and d) Hörby

2.2.3 Input to test design

The analysis in Section 2.2.2 indicates that water application rates of 72–138 l/m^2/h in the current standards [3, 7, 8] represent non-frequent WDR events in Sweden; probably realistic for high-rise buildings and may occur in a short period of time (i.e., not in the hourly scale). Thus, there is a need for a test setup capable of producing a more realistic range of WDR intensities encountered in Sweden to have a better understanding of masonry façade resistance to WDR. It is also clear that differential air pressure levels of 400–1000 Pa, applied in the test standards [3, 11, 12], are quite unlikely to act across the envelope in conjunction with rain.

Moreover, three WDR events taking around 21 h were recorded for Hörby during 1995 – 2020. Figure 5 shows the hourly WDR intensity for these three events, happening during 21 h of consecutive rainfall. The average WDR intensity for Hörby during these events is equal to 0.43 mm/h, 0.52 mm/h, and 0.68 mm/h. Additionally, the maximum hourly WDR intensity for each event is equal to 1.05 mm/h, 1.2 mm/h, and 2.25 mm/h. Therefore, based on the available results,

rain penetration tests of 46 hours and 90 hours with the water spray rate of 72 l/m^2/h and 120 l/m^2/h in accordance with NBI method 29/1983 [8] and NEN 2778 [7] represent extreme and non-frequent WDR events encountered in Sweden.

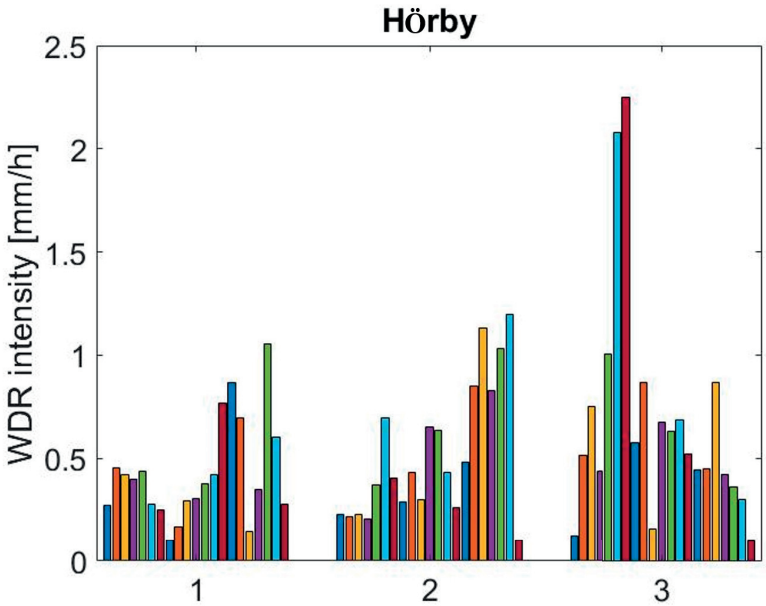

Figure 5. WDR intensity during three rainfall events with the duration of 21 h in Hörby during 1955-2020

2.3 Moisture transport

As moisture is one of the primary agents of damage and deterioration of façades, knowledge about moisture transport in building materials is of great importance. As in any porous material, free (liquid) water and vapor might co-exist in masonry. However, different phases of water are subjected to different mechanisms for transport through the material.

Many building materials, such as bricks and mortars, are hygroscopic, meaning they absorb or release moisture to the environment until equilibrium conditions are reached [59]. The relationship between moisture content and equilibrium relative humidity of building materials can be displayed in the form of so-called sorption-isotherms [60]. Figure 6 shows the absorption and desorption isotherms of typical clay brick and cement-based mortar. The steep slope at about 95% relative humidity can be referred to as the over-hygroscopic region of the sorption isotherm. In this region, water is absorbed mainly through capillary condensation. The moisture

content in bricks in the hygroscopic region is limited, normally below 10 kg/m^3, whereas it usually is several times higher in mortar.

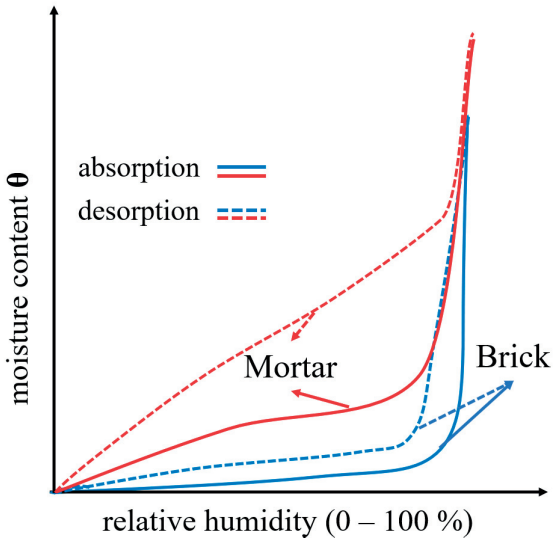

Figure 6. Sorption isotherms of typical clay brick and cement-based mortar

Although clay brick masonry façades absorb and release moisture to reach equilibrium with their ambient condition, the moisture content in this state is limited. Therefore, more attention is paid to moisture transport above the hygroscopic region, where capillary absorption dominates.

The transport mechanism of moisture depends on the phase of water and, as aforementioned, several phases of water co-exist in the pore system. The transport of water vapor is governed by diffusion and convection, whereas the transport of free water can be divided into unsaturated (capillary absorption) and saturated flow (permeation). While several transport mechanisms may occur simultaneously, the transport of free water becomes increasingly dominant as the material enters the over-hygroscopic region. It should be noted that masonry walls exposed to WDR generally do not attain full saturation throughout their depth. Transport of liquid water is thus, under normal circumstances, primarily governed by unsaturated flow through capillary absorption [57, 58].

2.3.1 Unsaturated flow

Since this study focuses on the resistance of masonry to driving rain, moisture transport in the liquid phase is in focus. Liquid transport in a single material, such as bricks or hardened mortar, is well understood and explained with capillary transport theory. Capillary absorption within capillary pores is mainly controlled by

the capillary pressure and can be analyzed by the so-called extended Darcy's equation, which can be written as follows:

$$u = -K(\vartheta) \times \nabla\varphi \quad (7)$$

where u is the flow rate within porous medium [m/s] and $K(\vartheta)$ is the liquid conductivity, also known as unsaturated permeability [m/s], a function of the normalized water content ϑ. The driving force, $\nabla\varphi$, is the gradient of the total hydraulic potential [-]. The hydraulic potential includes not only the capillary potential, Ψ [-], but also other external driving forces (such as external pressure and gravity). ϑ denotes the normalized water content [-] and can be calculated as follows [57, 58]:

$$\vartheta = \frac{\theta - \theta_r}{\theta_s - \theta_r} \;\&\; 0 \leq \vartheta \leq 1 \quad (8)$$

where θ is the volumetric water content [m^3], θ_r is the residual water content [m^3], and θ_s is the saturated water content [m^3].

A useful result that follows from Eq. (7) is an equation defining the advance of a water content profile as water is absorbed into an initially dry porous solid. When water is absorbed horizontally into an initially dry porous solid, all points on the waterfront advance as a function of the square root of time, $t^{1/2}$. In addition, the absorbed mass of water is proportional to the square root of time and can be written as follows.

$$m = \rho_w \, S \, A \, t^{1/2} \quad (9)$$

where m is the absorbed mass [kg], ρ_w is the density of water [kg/m^3], S is the sorptivity [$m/s^{1/2}$], and A is the cross-sectional area [m^2]. The sorptivity is an inherent property that describes the material's ability to absorb and transmit water by capillarity. Following Eq. (9), it is possible to determine how far the capillary front reaches as a function of time. The time, t [s], for the capillary front to reach a certain distance, z [m], in a porous medium may be calculated as follows:

$$t = \mu \, z^2 \text{ where } \mu = \left(\frac{p}{S}\right)^2 \quad (10)$$

where μ is the capillary resistance number [s/m^2], and p is the porosity [-].

While Eq. (10) is useful for describing the progression of a moisture front in a single material, masonry is made of both brick and mortar. Two materials that are in contact can transfer water through capillary action. In addition, an imperfect bond between brick and mortar can lead to reduced resistance to water along with the brick-mortar interface. Figure 7 illustrates, conceptually, the distribution of water in

clay brick masonry exposed to one-sided wetting under two different assumptions: a) full contact and b) water transport through the brick-mortar interface where it is assumed that the interface acts as a gap. Considering higher sorptivity for the brick in comparison with the mortar, it takes more time for the capillary front to reach a certain depth in the mortar than in the brick. In practice, water will be transported from the brick to mortar (Figure 7.a). Finally, if the capillary resistance of the interfacial zone is lower than that of brick and mortar, then the moisture distribution may conceptually be illustrated as shown in Figure 7.b.

It should be noted that in most instances of rain penetration in brick masonry walls, leakage occurs close to the brick-mortar interface, yet rain can pass through the bricks or the mortar joints under more unusual circumstances.

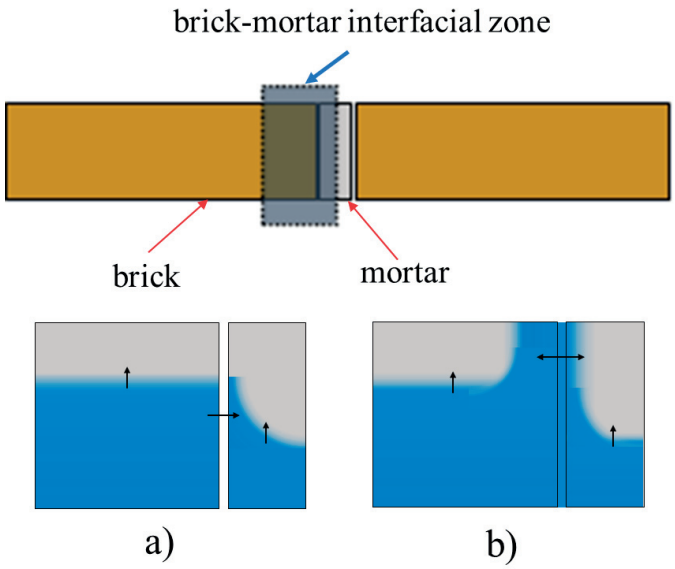

Figure 7. Moisture transport through a brick-mortar interfacial zone; a) full contact and b) lower capillary resistance

2.3.2 Saturated flow

The mathematical description for permeation of liquids through porous materials is based on Darcy's law, which can be written as follows [57, 62]:

$$Q = \frac{k \times A \times \Delta p}{\mu \times \Delta x} \qquad (11)$$

Where Q is the volumetric flow rate [m^3/s], k is the permeability [m^2], A is the cross-sectional area [m^2], Δp is the pressure gradient, i.e., the hydrostatic pressure

difference across the studied length, [Pa], μ is the dynamic viscosity [Pa.s], and Δx is the length [m] (Figure 8).

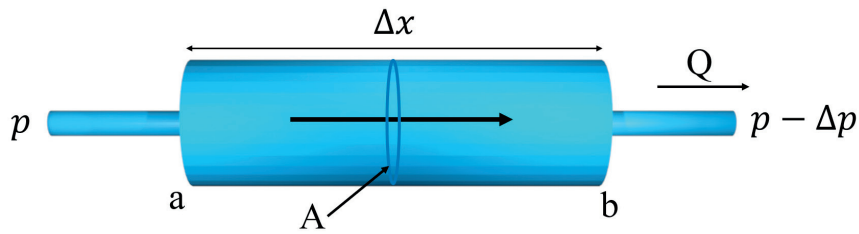

Figure 8. Simple Darcy flow through a liquid-saturated homogeneous medium under the action of a pressure gradient

By considering the hydraulic gradient applied between point a and b, $\nabla p = \Delta p/\Delta x$, Darcy's law is commonly written in terms of the flow rate or Darcy velocity, u [m/s], [57]:

$$u = \frac{Q}{A} = \frac{k \times \nabla p}{\mu} \text{ [m/s]} \quad (12)$$

The hydrostatic pressure is expressed as $p = \rho \cdot g \cdot h$; thus, Darcy's law can be written as follows:

$$u = \frac{k \times \rho \times g \times \partial h}{\mu \times \partial x} = \frac{K_s \times \partial h}{\partial x} \quad (13)$$

where ρ is the liquid density [kg/m^3] and g is the gravity [m/s^2]. The permeability coefficient, the saturated permeability of the material, K_s, is then described with the following equation [57, 63]:

$$K_s = \frac{k \times \rho \times g}{\mu} \left[\frac{m}{s}\right] \quad (14)$$

Permeation of liquid through porous materials is mainly relevant for studying moisture transport in cracked masonry, particularly in the head joints. It should be noticed that the pressure gradient to drive moisture into the brick masonry in this phase can be the hydrostatic pressure due to gravitational forces and wind imposing a differential air pressure.

2.3.3 Rain penetration of brick masonry façades

During WDR events, a thin water film may form on the exposed surface of the façades depending on the water absorption properties of masonry and WDR intensity. For rain penetration to occur, openings to permit rain penetration and

forces to drive or draw moisture inwards are required. It is clear that there are quite numerous openings on the face of a building in the form of pores, cracks, poorly bonded interfaces, and eroded mortar joints. Eventually, the main driving forces can be the capillary forces, gravity, and air pressure differences, leading to water penetration.

Birkeland [64] claims that water penetration occurs when cracks with 0.1 mm to 5 mm width exist; Grimm [65] categorizes existing interfacial cracks generally ranging between 0.1 and 1 mm. As mentioned above, the driving force for water to penetrate can be the air pressure difference induced by wind pressure, hydrostatic pressure due to gravity, and capillary suction in which for openings smaller than 0.5 mm, the capillary suction seems to be important. Considering that the surface tension of water is approximately 0.075 N/m, the capillary suction pressure for cracks in the range of 0.1 mm to 1 mm wide will be in the order of 75 to 750 Pa. It seems that even in the case of no air pressure difference between the exposed and protected surface, such considerable capillary suction pressures are sufficient to force water into the brickwork, i.e., no applied pressure (either hydrostatic or air) is required [66]. Additionally, significant hydrostatic pressure due to gravity can be built up in the existing interfacial cracks between the brick and mortar interface at the head joints, which may result in leakage [67]. The hydrostatic pressure of around 600 Pa may result from an interfacial crack between the brick and mortar over a typical brick with a height of 60 mm. Therefore, it seems that air pressure difference is not the primary cause of water penetration in brick masonry walls [68]. Further, water penetration in brick masonry specimens without any air pressure difference occurred in the experimental study presented in Paper III.

3 Methods and materials

Repointing of clay brick façades with eroded mortar joints is often motivated by higher water absorption and increased risk for water penetration from WDR. Nevertheless, knowledge concerning to what extent eroded mortar joints cause increased water absorption and penetration from WDR is limited. In this regard, a new test setup was developed to study the resistance of masonry to WDR, providing knowledge that can be applied to make a rational decision on repointing. As previously discussed in Section 2.2.3, the test conditions in the current standards represent extreme WDR conditions. Thus, the test conditions in the test setup presented in this study were adjusted to be more representative of frequently encountered WDR events in Sweden. Subsequently, the bricks and mortars used to prepare masonry specimens were characterized to determine water absorption properties, including the initial rate of absorption (IRA) and water absorption coefficient. Eventually, different types of masonry specimens built with different brick types and mortar joint profile finishes were considered.

3.1 Test setup

As WDR is a substantial source of moisture and a leading cause of mortar joints erosion, there is a need to study the resistance of clay brick masonry façade exposed to WDR. For water penetration to happen, driving forces can be one of the following forces: the kinetic force of raindrops, capillary forces, gravity, air pressure differences, and surface tension. Capillary forces and surface tension are a function of material properties, whereas kinetic forces and differential pressure are a function of the water application, which can be controlled in the test setups [69]. Several test setups are available in the literature [15, 70], aiming to study qualitatively or quantitatively water penetration in masonry walls. A comparative study reviewing the effectiveness of existing water penetration and leakage tests, conducted by Driscoll and Gates [15], identifies a need for a simple test method to complement existing ones since little attention has been given to the correlation between tests and the factors that contribute to water penetration.

Accordingly, a new test setup was developed to study a more realistic behavior of masonry exposure to WDR events. The test setup is able to produce a uniform water spray covering the exposed surface of masonry specimens. A uniform and well-

distributed water spraying pattern was achieved using a low flow, full cone BETE WL nozzle (WL – 1/4, Full Cone, and 90° Spray Angle). It is possible to apply a wide range of water spray rates and air pressure levels, simulating different driving rain intensities. The test setup is equipped with two water pressure regulators and a water flow meter to control the water spray rate. Additionally, two digital scales are employed to measure water absorption and water penetration continuously. A digital camera mounted on the protected side of the specimens traces the appearance and spread of damp patches. Figure 9 shows the schematic of the test setup.

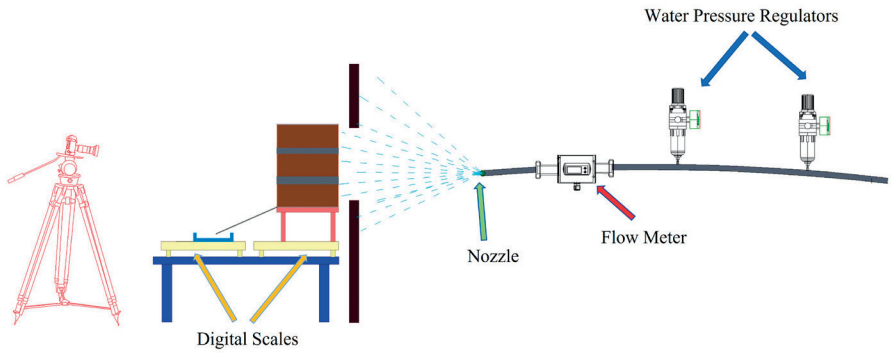

Figure 9. Schematic of the test setup

The following aspects were taken into account to develop the presented test setup: a) a nozzle producing low water flow with a full cone spray pattern was used, and b) the distance between the surface of the specimens and the nozzle was adjusted to assure a uniform coverage of the exposed surface. The droplet size of the water spray concerning quality and uniformity was examined visually using a paper towel placed in the frame opening and exposed to the water spray for 1-2 seconds, as shown in Figure 10. A more detailed description of the test setup is presented in Paper II and III.

Figure 10. Wet dots on a paper sheet exposed to water spray for 1–2 seconds.

Two improvements in the developed test setup were achieved in comparison with the currently existing test setups. First and foremost, the continuous measurement of the water absorption (mass gain) provides adequate knowledge concerning moisture content of masonry and a basis for analyzing the hygrothermal performance of a building envelope. Secondly, the exposed surface of the specimen is uniformly covered with water drops, unlike other test methods in which the surface of the masonry is kept covered with a thin layer of water film from a pipe/nozzle placed close to the upper part of the specimen. The high water spray rates and differential air pressure used in many standards are to assure that a water film is formed from the beginning of the exposure, allowing water penetration to take place before saturation of the masonry. This means that the influence of the water absorption capacity of the specimen is neglected [67]. Neglecting buffering capacity of masonry gives a misleading picture of clay brick masonry response to WDR exposure.

3.2 Test conditions

It can be observed in the literature that the ASTM E514 [3] standard is one of the most frequently used test methods in studies to investigate water penetration through masonry walls. However, the test conditions of ASTM E514 [3] standard represent extreme driving rain conditions that can only occur at specific locations, with very low probabilities, as analyzed by Fishburn et al. [71] and Cornick and Lacasse [72]. Furthermore, Ribar [6] suggests that current test standards need to be revised to incorporate a realistic exposure condition approach. Additionally, the range of WDR events in Sweden, as shown in Figure 3, indicates that the water application rate of 138 l/m^2/h and differential air pressure of 500 Pa is extreme for the Swedish climate. Moreover, according to the field measurements and literature review done by Straube and Burnett [66], driving rain deposition rates of more than 5 – 10 l/m^2/h are only very rarely encountered, even on tall buildings. Eventually, Sandin [73] recorded a maximum WDR intensity of about 6 l/m^2/h during an observation period lasting 26 months in Gothenburg, Sweden.

Consequently, the primary considered criterion to develop the test setup was lowering the water spray rate compared with the test conditions of ASTM E514 [8] to represent a more realistic range of WDR events. In doing so, in the first experimental campaign, presented in Section 3.3.3, the tests were conducted at zero differential air pressure, at water spray rates varying between 1.7 and 3.8 l/m^2/h, representing WDR intensities frequently encountered in Sweden (see Figure 3) and approximately 95% lower than the water application rate specified in current standards [3, 7, 8]. In order to obtain the targeted low water spray rates, different combinations of water pressure and nozzle-to-specimen distances were tested. To arrive at the water spray range used in the first campaign, a pressure of 0.55 bar and

a nozzle–to–specimen distance of 55 cm were eventually chosen. Retrospectively, choosing a water pressure of 0.55 bar was not optimal since the recommended operating range of the nozzle is between 0.7 – 20 bars. The flow and thus the water spray became more sensitive to changes in the water pressure.

In the second experimental campaign, presented in Section 3.3.3, to minimize water flow variations and better control the water spray rate, water pressure was adjusted to nearly 1.05 bar, and nozzle–to–specimen distance decreased to roughly 50 cm. Thus, the tests were performed in this campaign with a water spray rate of 6.3 l/m^2/h ± 5 % and zero differential air pressure. A water spray rate ranging between 5 and 10 l/m^2/h was considered by Straube and Brunett [67] as representative for more realistic WDR events.

In both experimental campaigns, triplet masonry specimens were tested over a period of 23 hours, including six consecutive cycles; each cycle consisted of 210 min of water spraying and 20 min of drying. It should be mentioned that the tests were carried out with zero differential air pressure because high wind speeds usually occur only for a small percentage of rain duration, whereas in this study, the specimens were subjected to water spraying for 21 h.

3.3 Materials

3.3.1 Bricks

Three different types of commonly used solid clay bricks on the Swedish construction market, supplied by Wienerberger AB, were considered in this study, named bricks type I, II, and III. Twenty bricks from each type were tested to characterize the initial rate of absorption (IRA) and 24-h water absorption properties; tests were carried out as described in the ASTM C67 standard [74]. The IRA represents the surface absorption rate when the brick just contacts water, whereas the 24-h water absorption represents the amount of water that a brick can absorb when fully immersed in water, expressed as the ratio between the absorbed water and the initial weight. The average IRA of bricks type I, II, and III is equal to 1.95 kg/m^2, 1.81 kg/m^2, and 0.71 kg/m^2, respectively, whereas 24-h water absorption property amounts to 16.0 %, 8.6 %, and 4.0 %, respectively. According to the results of the IRA test, bricks type I and II can be classified as medium suction bricks [I] and [II], while bricks type III are considered low suction bricks. Table 1 summarizes the properties of bricks, including density, IRA, and 24-h water absorption.

Table 1. Material properties of bricks and mortars including density, IRA, 24-h water absorption, and water absorption coefficient (A_w)

Materials	Dimensions ($mm \times mm \times mm$)	Density ρ (kg/m3)	Average IRA ($kg/m^2/min$)	CoV (%)	Average 24-h water absorption (%)	CoV (%)	Average A_w (kg/(m^2.s$^{0.5}$))	CoV (%)
Brick type I	250×120×62	1800	1.95	2.3	16.0	1.6	0.193	0.8
Brick type II	250×120×62	1990	1.81	5.1	8.6	14.5	0.133	16.1
Brick type III	240×115×62	2235	0.71	13.7	4.0	38.6	0.042	22.8
Mortar M 2.5	100×100×100	1869	0.30	15.8	-	-	0.022	8.7
Mortar NHL 3.5	100×100×100	1715	0.80	20.4	-	-	0.159	9.2
Mortar NHL 5	100×100×100	1733	1.10	15.6	-	-	0.236	15.3

Moreover, tests to determine the water absorption coefficient of bricks, A_w, were done on ten bricks from each type according to the ASTM C1403 – 15 standard [75]. The water absorption coefficient, A_w, expresses the rate of capillarity action in a certain time. Bricks were immersed in water at a depth of 3-5 mm from the bed face, and the weight was measured at different time intervals. The increase in mass as a result of water absorption was registered after 1, 5, 10, 20, 30, 60, 120, 180, 240, 300, 360, 1440, and 4320 minutes. The amount of absorbed water per unit area of the brick Q [kg/m^2] is defined as the ratio between the difference of increased weight (w_i [kg]) and initial weight (w_0 [kg]) and the cross-sectional area of the brick A [m^2] (Eq. (15)).

$$Q = \frac{w_i - w_0}{A} \ [kg/m^2] \qquad (15)$$

To present the results of the tests, Q [kg/m^2] is plotted against the square root of time [s$^{1/2}$] (Figure 11.a). Eventually, the water absorption coefficient, A_w [kg/(m^2.s$^{0.5}$)], is mathematically defined as the tangent to the initial, linear branch of the Q – t$^{1/2}$ function (Figure 11.b). The average water absorption coefficient for each type of brick is presented in Table 1.

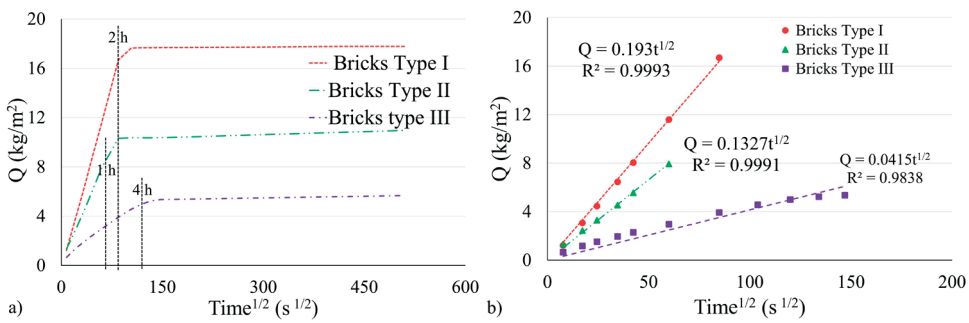

Figure 11. Plot of the average water absorption per unit area against the square root of time for ten masonry brick units from each type (bricks type I, II, & III): a) up to 72 h; and b) during the initial stage of the test.

3.3.2 Mortars

Mortar M 2.5, widely used in masonry façades, was supplied by Weber Saint-Gobain AB; Natural hydraulic lime (NHL) 3.5 and 5 mortars, commonly used for repointing of clay brick façades, were supplied by Målarkalk AB. The recommendation was to use NHL 3.5 with high and medium suction bricks, whereas NHL 5 mortar is recommended to be used with low suction bricks. Eighteen 100 mm cubic side mortar specimens, including 12 M 2.5, 3 NHL 3.5, and 3 NHL 5, were cast to characterize the water absorption properties of mortars. The water absorption coefficient of the mortars was determined according to the ASTM C1403 – 15 standard [75]. Figure 12 shows the water absorption rate of the mortars over the square root of time, and Table 1 summarizes the average IRA and water absorption coefficients of three different types of mortar.

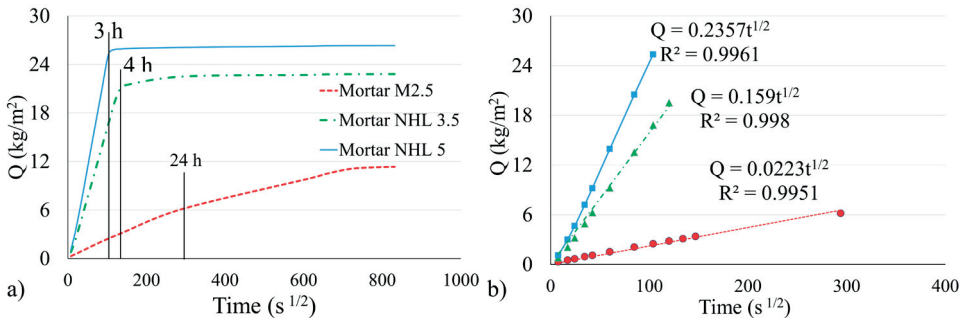

Figure 12. Average water absorption of mortar M 2.5, NHL 3.5, NHL 5: a) up to 8 days; and b) during the initial stage of the test

3.3.3 Masonry specimens

Three different types of bricks with different water absorption properties and two different mortar joint profiles, namely flush and raked, were considered. Flush profiles were subdivided into standard and after-pointed. After-pointing is a common technique in Nordic countries in which the joints are filled with mortar; then, prior to hardening of the mortar, the outer part is removed; and a couple of hours later, the remained part is finally filled with repointing mortar and tooled. Raked specimens can be a reasonable representative of eroded mortar joints. Comparing water absorption and penetration of flush and raked specimens can facilitate understanding how the erosion of the mortar joints might affect WDR-related water absorption and penetration.

The tests were carried out on triplet masonry specimens with the length, height, and depth of 250 ± 5 mm, 215 ± 3 mm, and 120 ± 2 mm, respectively, see Figure 13. The specimens were intended to be representative of a masonry veneer wall. The

specimen size was limited to three bricks in order to facilitate manual handling without damaging either the specimens or the operator. A similar choice was made by Ritchie [13], who studied water penetration in brick masonry by using specimens consisting of five bricks, yet without any head joints.

As summarized in Table 2, in the first campaign (A), 39 triplet masonry specimens were prepared with medium suction bricks type [I] and [II], with three types of joint profile finish: flush, raked, and after-pointed. In the second campaign (B), 36 masonry specimens, built with three different types of bricks, including medium suction bricks type [I] and [II], and low suction bricks, type III, and three different types of joint profile finishes, including flush, raked, and after-pointed were studied. All specimens in the two campaigns were prepared at the same time.

Specimens built with medium suction bricks [I] belong to Series I, whereas Series II consists of specimens prepared with medium suction bricks [II]. Series III includes specimens built with low suction bricks, type III. Each Series is then divided into three groups based on the joint profile finish. Group G1 includes specimens built with mortar M 2.5 with a tooled flush joint profile, whereas group G2 consists of specimens built with mortar M 2.5, with a raked joint profile. Group G3 is also made up of specimens built with mortar M 2.5, but compared with G1, the outer 6 mm of the mortar joint was pointed one day after bricklaying with mortar NHL 3.5 or NHL 5, with a tooled flush joint profile. It should be mentioned that mortar NHL 3.5 was used in the pointing of Series I and II specimens, whereas NHL 5 was used in combination with the specimens of Series III, low suction bricks.

Following the recommendations of the supplier, the bricks were not wetted before bricklaying. These recommendations are in line with those given in [76] concerning the need for pre-wetting bricks as a function of the IRA. To eliminate uncertainties regarding workmanship, a single craftsman built all the specimens. Extra effort went into ensuring that the same amount of water was added to each batch of mortar mix, i.e., eliminating the effect of mortar flow on water penetration. Specimens of group G1, with mortar M 2.5, were tooled with a wooden stick to have a flush profile. For specimens with the raked joint profile, group G2, a 5 mm screw was used to remove extra mortar to reach the depth of 5 mm. For specimens prepared with the after-pointing technique, the excess mortar was removed using a 6 mm screw, and the following day, the 6 mm gap was filled with either NHL 3.5 or NHL 5 and tooled to have a flush joint profile (Figure 13). The workmanship technique used for bricklaying in this study was the so-called pushing of the head joints. Figure 13.c shows the backside of the representative specimens.

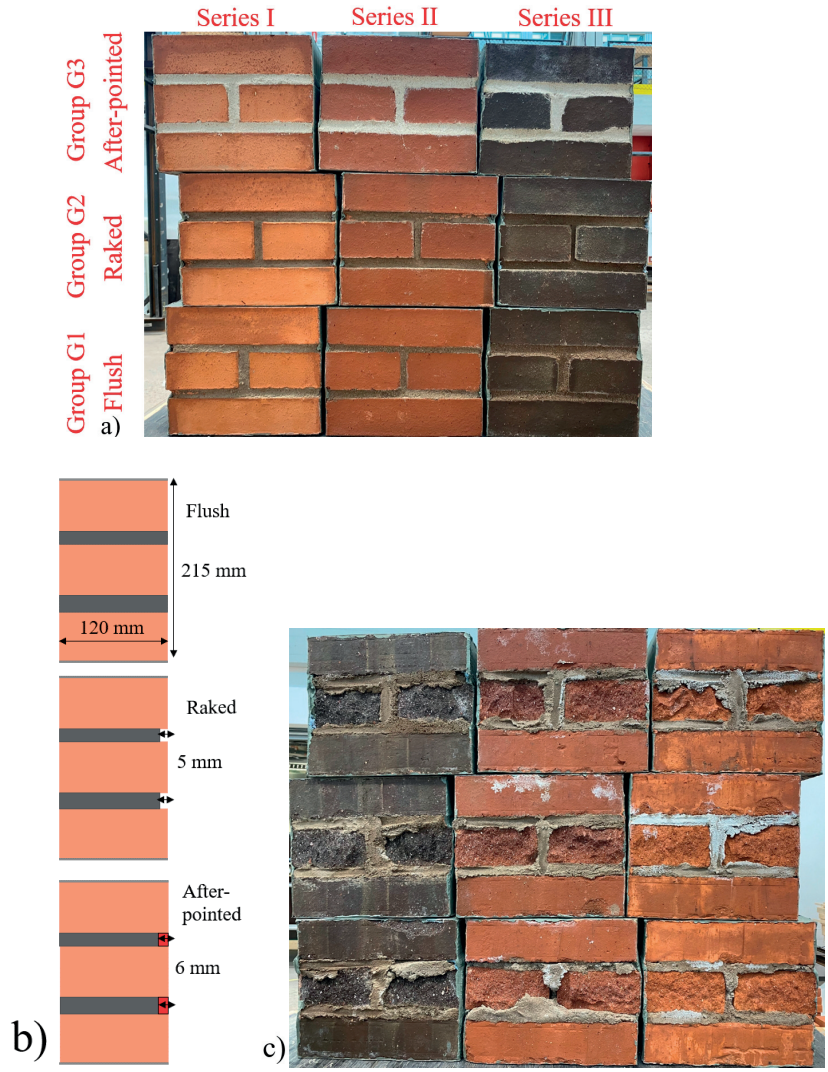

Figure 13. a) Representative specimens from each group and Series after sealing; b) Schematic of the mortar joint profile finishes, and c) Backside of representative specimens

Prior to the testing, all sides except the exposed surface and backside of the specimens were sealed using a two-component sealant (ARDEX P2D and ARDEX S1-K), producing a flexible waterproof coating. The sealing was done to avoid any undesirable water absorption in any other sides except the exposed surface.

The specimens were named following the designation W-X-T-C, where W stands for the experimental campaign (A is the first campaign, B is the second campaign),

X represents the Series (I is the first Series, II is the second Series, III is the third Series), T corresponds to the mortar joint profile finish (F = flush, R = raked, AF = after-pointed), and C refers to the specimen number. For example, specimen A-II-R-2 is one of the specimens tested in the 1st experimental campaign, was built with medium suction bricks type [II], with a raked joint profile, and it is the second specimen of group G2.

Table 2. Specimen designation and configurations

Experimental campaign	Series	Group	Brick	Mortar	Joint profile finish	Ave water spray rate (l/m²/h)	No. of specimen
First campaign A	Series I	G1	Medium suction type [I]	M 2.5	Flush	3.6	5
		G2	Medium suction type [I]	M 2.5	Raked	3.6	5
		G3	Medium suction type [I]	M 2.5 / NHL 3.5	After-pointed	3.4	5
	Series II	G1-a	Medium suction type [II]	M 2.5	Flush	3.2	5
		G1-b	Medium suction type [II]	M 2.5	Flush	2.0	3
		G2	Medium suction type [II]	M 2.5	Raked	2.3	8
		G3	Medium suction type [II]	M 2.5 / NHL 3.5	After-pointed	2.0	8
Second campaign B	Series I	G1	Medium suction type [I]	M 2.5	Flush	6.3	4
		G2	Medium suction type [I]	M 2.5	Raked	6.3	4
		G3	Medium suction type [I]	M 2.5 / NHL 3.5	After-pointed	6.3	4
	Series II	G1	Medium suction type [II]	M 2.5	Flush	6.3	4
		G2	Medium suction type [II]	M 2.5	Raked	6.3	4
		G3	Medium suction type [II]	M 2.5 / NHL 3.5	After-pointed	6.3	4
	Series III	G1	Low suction	M 2.5	Flush	6.3	4
		G2	Low suction	M 2.5	Raked	6.3	4
		G3	Low suction	M 2.5 / NHL 5	After-pointed	6.3	4

In the first campaign (A), the specimens in groups G1, G2, and G3 of Series I were exposed to an average water spraying rate of 3.6, 3.6, and 3.4 l/m²/h. Specimens of group G1 of Series II are divided into two groups, G1-a and G1-b, based on the average water application rate. In this regard, the average water spraying rate for groups G1-a, G1-b, G2, and G3 of Series II was 3.2, 2.0, 2.3, and 2.0 l/m²/h, respectively (Table 2). However, in the second campaign (B), all specimens were exposed to a uniform and constant water spray rate of 6.3 l/m²/h ± 5% (Table 2). It should be noted that the first campaign includes only Series I and II specimens, whereas the second campaign consists of all specimens of Series I, II, and III.

4 Experimental results

This chapter presents the results of two experimental campaigns and is divided into four subsections: general observations, water absorption, damp patches, and water penetration. In the first part, observations and qualitative results regarding the response of specimens exposed to water spray, observed during testing, are presented. Section 4.2 summarizes the experimental test results regarding the water accumulation and moisture content of the specimens. Section 4.3 provides information about the appearance and spread of damp patches on the backside of the specimens. Section 4.4 indicates the amount of water that was collected from the backside of specimens due to leakage.

4.1 General observations

This part presents the obtained qualitative results, including water absorption behavior, surface saturation, the appearance of damp patches, and water penetration observed during the testing of the specimens. Firstly, the specimens were exposed to a water spray, with a rate controlled by two water pressure regulators. At the beginning of the test, the specimens absorbed most of the sprayed water, whereas the rest of the water drops bounced off.

Afterward, runoff started on the exposed surface of the specimens, indicating that surface saturation was attained. The time to attain surface saturation varied between different specimens, depending on the water spray rate and the water absorption coefficient of the bricks. Subsequently, the first visible damp patches usually appeared on the backside of the specimens in the vicinity of the head joint. It should be noted that for a few specimens of Series III, the first dampness was observed soon after starting the test. Subsequently, the dampness spread on the entire second course, including the head joint. Then, the bottommost course became damp. The dampness eventually spread to the uppermost course until the entire protected side of the specimen became damp. However, the backside of a few specimens within Series III did not get fully damp.

The absorption then continued until the specimens reached full saturation, depending on the water spray rate, the water absorption coefficient of bricks, and the water absorption capacity of masonry. However, several specimens did not reach

full saturation, mostly because of the low water spray rate and low water absorption properties of masonry. In the first experimental campaign (A), due to the low water spray rate, the amount of water collected from the backside of the specimens, the water penetration, was limited. Thus, water penetration was only registered in the second campaign (B), where the water spray rate increased compared to the first campaign (A). In most specimens, water penetration started when the specimens were close to saturation. Water penetration mainly occurred through the brick-mortar interface, particularly the bed joint between the first and the second course.

4.2 Water absorption

As the developed test setup was equipped with a scale capable of measuring the amount of absorbed water continuously during the test, in this section, the results of water absorption in specimens tested in the first (A) and second (B) experimental campaigns are presented.

4.2.1 First campaign (A)

It should be mentioned that individual specimens in campaign A were exposed to water spray rates varying between 1.7 and 3.8 l/m^2/h. The water absorption, Q [kg/m^2], herein is defined as the amount of absorbed water [kg] per unit area of the masonry specimen [m^2]. Figure 14 shows the absorption behavior of masonry specimens during 23 h of testing, tested in the first experimental campaign (A). Since the water spray rate of Series II group G1-a is similar to those of Series I, they are plotted in the same graph (see Figure 14.a). It should further be kept in mind that the specimens in Series I and Series II Group G1-a were exposed to a more intensive spray rate (3.2 – 3.6 l/m^2/h) than the specimens in Series II group G1-b, G2, and G3 (2.0 – 2.3 l/m^2/h).

It is clear that during the 1st cycle (3.5 h), the absorption behavior is linear, indicating that most of the sprayed water was absorbed within the specimens. Accordingly, the absorption behavior of Series II group G1-a during the first cycle is similar to those of Series I specimens, yet with different absorption properties of the bricks. Hence, it can be seen that the absorption during the first cycle, prior to surface saturation, is strongly dependent on the water spray rate. Similarly, the absorption behavior of Series II group G1-b, G2, and G3 during the first cycle is similar to each other (Figure 14.b), indicating that the water spray rate is the governing agent influencing the amount of absorbed water. The slight difference in the amount of absorption after the 1st cycle is related to the difference in the water spray rate; the greatest absorption was recorded in group G2 exposed to an average spray rate of 2.3 l/m^2/h,

in comparison with group G1-b and G3 exposed to the average water spray rate of 2.0 l/m^2/h.

It was mentioned that a large portion of the sprayed water during the first cycle was absorbed within specimens. Since the absorption behavior is linear during the first cycle, i.e., surface saturation is not attained yet, the difference between the amount of sprayed water and absorbed water can be considered as bounce-off. Therefore, around 8 – 23 % of the sprayed water is considered to have bounced off from the specimens' surface.

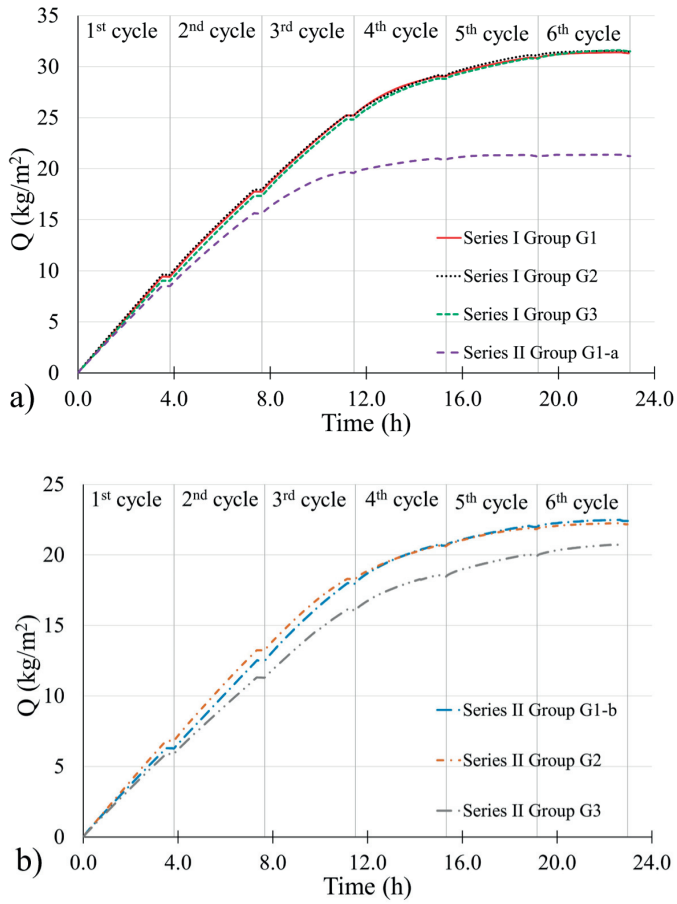

Figure 14. Average water absorption vs. time response of a) Series I and Series II group G1-a; b) Series II group G1-b, G2, and G3 in the first experimental campaign (A)

As the test progressed, the absorption behavior became nonlinear, indicating saturation of the exposed surface. The time to attain surface saturation is dependent on the water spray rate and water absorption coefficient of the masonry. Accordingly, surface saturation was attained later for Series I in comparison with

Series II group G1-a, indicating that a higher water absorption coefficient allows rapid moisture transport and postpones saturation of the exposed masonry surface layer, as stated by Van Den Bossche et al. [17] and further discussed in Paper II. Surface saturation was attained at the end of the 3rd cycle for all groups of Series I and II, except Series II group G1-a in which the absorption curve becomes nonlinear at the end of the 2nd cycle. Once the surface saturation was attained, a water film was formed on the exposed surface of the masonry, and the absorption behavior became more dependent on the water absorption coefficient and water absorption capacity of the masonry.

Eventually, as can be seen, the absorption continues until the middle of the 6th cycle for Series I, showing the specimens are close to fully saturated. However, for Series II groups G1-b, G2, and G3, the absorption continues until the end of the test, mainly attributed to the relatively low water spray rate. In contrast, the absorption ends during the 5th cycle for Series II group G1-a, indicated by the slope of the Q – t curve becoming close to zero (i.e., nearly no water accumulation in the specimens) during the remainder of the test.

4.2.2 Second campaign (B)

Figure 15 shows the average amount of water absorption, Q [kg/m^2], during 23 h of testing in all groups within Series I, II, and III tested in the second experimental campaign (B). It should be noted that all specimens were exposed to a uniform and constant water spray rate of 6.3 l/m^2/h ± 5%. During the initial 10 minutes to 2 hours of tests, depending on the Series, most sprayed water was absorbed, indicating that surface saturation was not attained yet. The bounce-off varied between 7 % and 14 %.

Surface saturation for Series I and II were attained after around 1 h and 2 h, respectively. In contrast, the occurrence of surface saturation took only 10 minutes for Series III, as shown in Figure 15.b. Once the surface saturation was attained, which can be seen from the deviation from a linear slope of the absorption curve, the absorption response becomes nonlinear. The time to reach surface saturation varied between each Series depending on the water absorption coefficient of the bricks. It can be observed that surface saturation was attained during the 1st cycle for all groups, G1, G2, and G3, within each Series, though it took more time for Series I, specimens prepared with bricks with the absorption coefficient of 0.193 kg/(m^2.s$^{0.5}$), in comparison with Series II and III, built with bricks with the absorption coefficient of 0.133 kg/(m^2.s$^{0.5}$) and 0.042 kg/(m^2.s$^{0.5}$), respectively.

After the attainment of surface saturation in specimens of Series I and II, the absorption behavior becomes nonlinear, and the slope of the curve decreases until the point where it becomes close to zero, i.e., nearly no water accumulation in the specimens. The absorption ends during the 4th cycle for Series I and II, specimens

prepared with medium suction bricks type I and II. In contrast, once the surface saturation was attained at the beginning of the 1st cycle for Series III, the absorption behavior became nonlinear and continued until the end of the test. Based on the obtained results, the water absorption rate in masonry specimens during 23 h of the test depends on the water absorption coefficient of the bricks and water spray rate, whereas the total amount of water absorption is mostly correlated to the absorption capacity of the masonry.

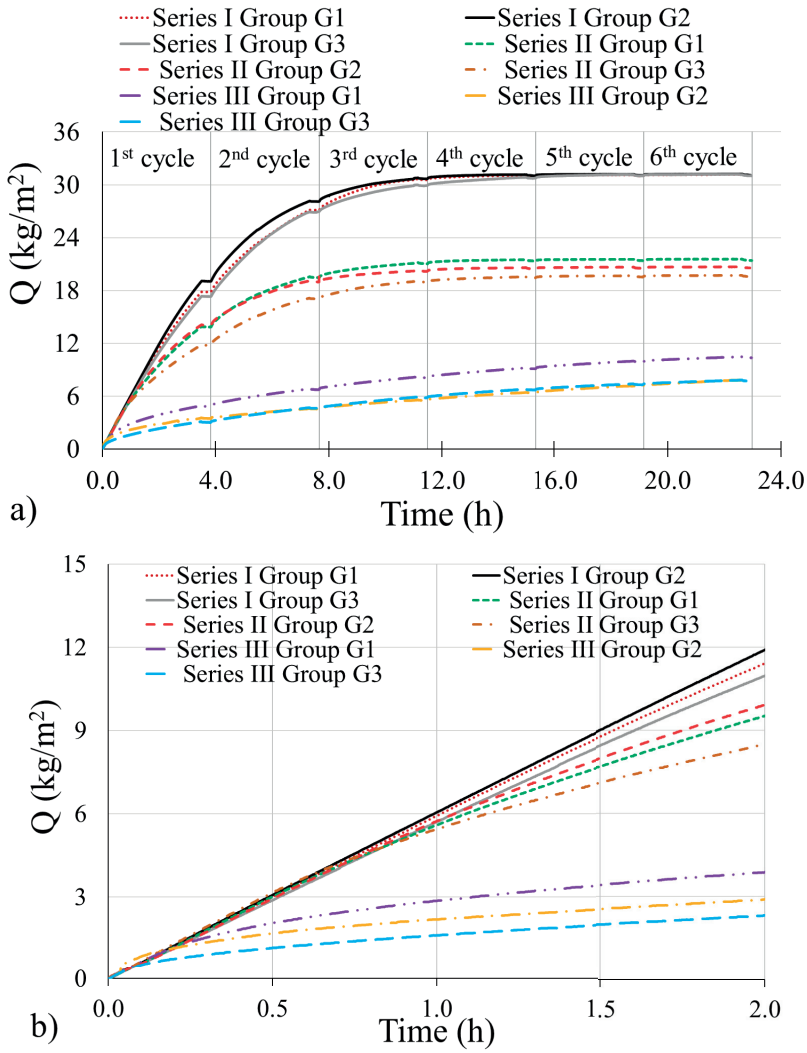

Figure 15. Average water absorption vs. time response of Series I, Series II, and Series III in the second experimental campaign (B), a) during 23 h of testing and b) during the first two hours after starting the test

Table 3 summarizes the average amount of water absorption, Q [kg/m2], within each group after performing the first and sixth cycles. Based on the obtained results in campaign A, the water absorption in the first cycle is dependent on the water spray rate. For instance, in Series II, the lowest average water absorption, amounting to 5.9 kg/m^2, is exhibited by group G3, exposed to the lowest average water application rate of 2.0 l/m^2/h. Similarly, group G1-a, which was exposed to the highest average water application rate of 3.2 l/m^2/h, has the highest average water absorption of 8.5 kg/m^2 in Series II. However, in campaign B, as specimens were exposed to the same water spray rate, 6.3 l/m^2/h, the slight difference in the amount of water absorption after the 1st cycle for each group within each Series might be related to the; a) variability in brick absorption properties, b) effect of mortar joint profile finish, and c) variation in the applied spray rate, taking into account a mentioned tolerance of 5 % in the spray rate.

Table 3. The average water absorption and time to the appearance of the first visible damp patch on the backside of each group within each Series in Campaign A and B after the first and the sixth cycle

		Ave water spray rate (l/m^2/h)	Ave 1st cycle Absorption (kg/m^2)	Ave Total Absorption (kg/m^2)	CoV %	Time to the 1st dampness (h)
Campaign A	Series I group G1	3.6	9.4	31.3	0.6	7.9
	Series I group G2	3.6	9.6	31.5	0.3	7.8
	Series I group G3	3.4	9.0	31.5	0.2	8.0
	Series II group G1-a	3.2	8.5	21.2	10.4	4.8
	Series II group G1-b	2.0	6.3	22.4	6.3	6.3
	Series II group G2	2.3	6.8	22.2	6.0	5.9
	Series II group G3	2.0	5.9	20.6	5.6	6.4
Campaign B	Series I group G1	6.3	17.8	30.9	0.9	2.5
	Series I group G2	6.3	19.0	30.9	0.5	2.6
	Series I group G3	6.3	17.3	31.0	0.7	3.7
	Series II group G1	6.3	13.8	21.4	10.0	2.0
	Series II group G2	6.3	14.0	20.5	10.4	1.5
	Series II group G3	6.3	11.8	19.6	2.7	3.1
	Series III group G1	6.3	4.8	10.4	19.3	1.0
	Series III group G2	6.3	3.5	7.7	10.1	6.9
	Series III group G3	6.3	3.1	7.7	30.3	3.6

It can be seen that the average total absorption in specimens of Series I, tested in the first (A) and the second (B) experimental campaigns, is nearly equal to 31.0 kg/m^2, highlighting a negligible difference in the average water absorption between groups G1, G2, and G3. In contrast, the average water absorption for groups G1, G2, and G3 of Series II varied between 20.6 kg/m^2 and 22.4 kg/m^2 in campaign A and between 19.6 kg/m^2 and 21.4 kg/m^2 in campaign B. The obtained results indicate a strong correlation between the total amount of absorption and the absorption capacity of the masonry. The difference in the results of average water absorption between each group in Series III is mainly attributed to the high variability in the water absorption capacity of the bricks (CoV = 38.6 %).

According to the obtained results, water absorption is not dependent on the joint profile finishes, suggesting that the impact of eroded mortar joints on water absorption from WDR is inconsiderable. In contrast, water absorption in clay brick masonry is a function of the water absorption properties of masonry, especially that of the bricks, and the water spray rate. The obtained results from specimens prepared with raked joint profiles as representative of eroded mortar joints may provide the basis for the decision-makers concerning repointing. Eroded mortar joints may not lead to a significant increase in water absorption in masonry façades built with solid clay bricks.

4.3 Damp patches

A digital camera was mounted behind the specimens in the presented test setup, providing the opportunity to obtain the location of the first visible dampness and the relative damp area over time. Figure 16 shows the location of the first visible damp patch on the backside of the specimens tested in the first campaign (A). It can be seen that the first dampness appeared close to the brick-mortar interface, indicating that the interfacial zone between brick and mortar is the primary path for water penetration.

Figure 16 and Table 3 summarize the time to the appearance of the first damp patch on the backside of the specimens. In the first campaign (A), the average time to the appearance of the first dampness for all groups of Series I is around 8 h, highlighting the insignificant effect of joint profile finish. In Series II, the dampness appeared after 4.8 h on the backside of group G1-a specimens with the water spray rate of 3.2 l/m^2/h, whereas it took nearly 6.4 h for group G1-b and G3 specimens exposed to the water spray rate of 2.0 l/m^2/h, suggesting the considerable effect of water spray rate on the appearance of the first damp patch. Moreover, comparing the time to the appearance of the first damp patch between all groups of Series I and group G1-a Series II, though specimens were exposed to a similar water spray rate, the obtained

results indicate the impact of brick absorption capacity on time to the appearance of the first dampness.

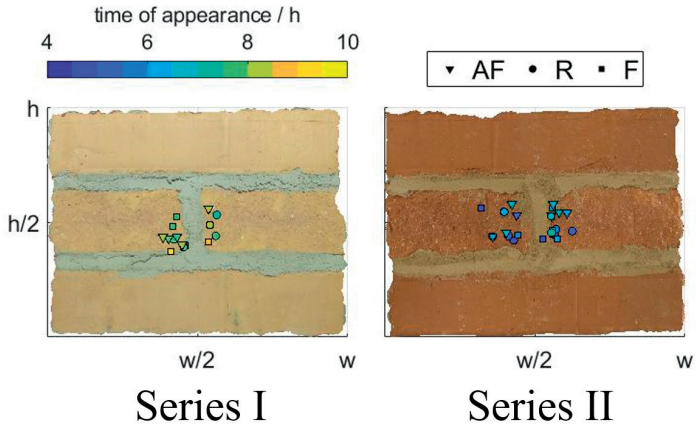

Figure 16. Location and time to the appearance of the first damp patch on the backside of specimens in campaign A

Figure 17 shows the time and location of the first visible dampness that appeared on the backside of specimens tested in the second campaign (B). Similar to the first campaign (A), with some exceptions, the first visible dampness appeared close to the brick-mortar interface in the vicinity of the head joint. Additionally, for those specimens where the dampness did not appear in the vicinity of the head joint, the time to the appearance of the first damp patch is significantly postponed. Accordingly, the obtained results indicate the importance of the resistance of the brick-mortar interface, particularly the head joint, to WDR.

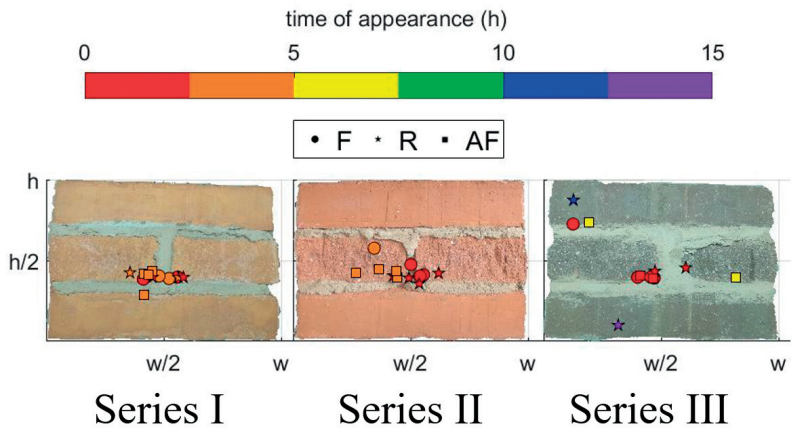

Figure 17. Where and when the first damp patch appeared on the backside of specimens in campaign B

Once the first damp patch appeared, mainly in the vicinity of the head joint, then typically it spread on the entire second course, including the head joint. Subsequently, the bottommost course became damp. The dampness eventually spread to the uppermost course until the entire protected side of the specimen became damp, as shown in Figure 18. However, it was observed that the backside of several specimens within Series III, specimens prepared with low suction bricks, did not reach even 50 % dampness after 21 h of water spray exposure.

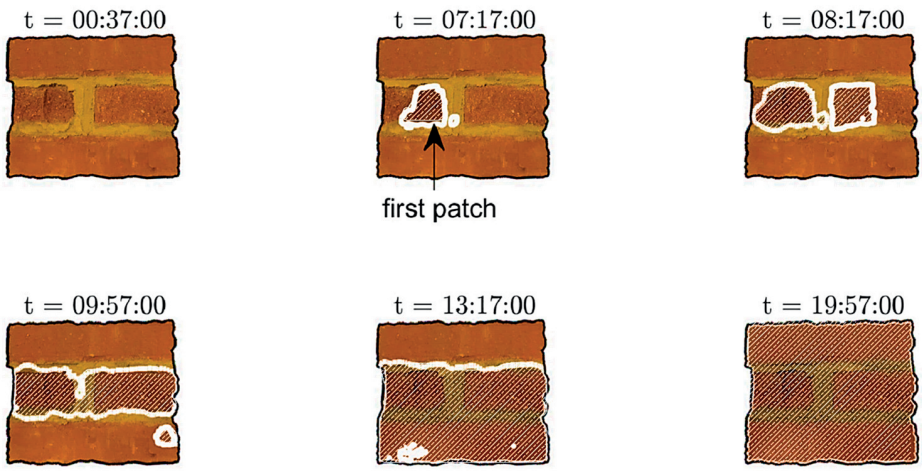

Figure 18. Appearance and growth of dampness on the backside of specimen A-II-F-6 at different time intervals.

The obtained results highlight the importance of the workmanship and a well-established contact between brick and mortar, as it may increase the time to the appearance of the first dampness and change its location. Additionally, the results reveal the low resistance of head joints to WDR, which might be related to the difficulty of the workmanship in filling the head joints and low compaction in comparison with bed joints [82]. Further, the effect of joint profile finishes on the time and location of the first visible dampness is negligible, whereas water spray rate and water absorption properties of bricks may strongly influence the time to the appearance of the first damp patch.

4.4 Water penetration

As no considerable amount of water leakage that could be collected from the backside of the specimens was observed in the first experimental campaign (A), this section only presents the results of water penetration in specimens tested in the second experimental campaign (B).

In the test setups of current standards and research studies, high water spray rate and air differential pressure are applied to rapidly form a water film on the exposed surface of the specimens and force the water in without gaining the benefit from the storage capacity of masonry [67]. In contrast, in the first campaign (A) conducted in this study, because of the low water spray rate and zero differential air pressure, no considerable amount of water penetration could be collected, indicating that the specimens could absorb most of the sprayed water. The limited leakage is probably due to the fact that specimens in campaign A got saturated at the end of the test. Thus, gravity is the probable driving force, see Section 2.3.3.

The average amount of water penetration [kg/m^2] for each group within each Series during 23 h of testing is shown in Figure 19 and Table 4. It can be seen that water penetration in all groups within Series I and II started at the end of the second cycle or the beginning of the third cycle, indicating that it started when the masonry specimens were nearly close to saturation, as already noted by Straube and Burnett [67]. Further, it is observed that for Series III, specimens prepared with low suction bricks, a lower value of water penetration was recorded in comparison with Series I and II. In this regard, the average amount of penetrated water of groups G1, G2, and G3 of Series I and II are in the range of 2.0 kg/m^2 – 4.4 kg/m^2. In contrast, there is no considerable water penetration for specimens of Series III, except specimen B-III-F-1, B-III-AF-2, and B-III-AF-3.

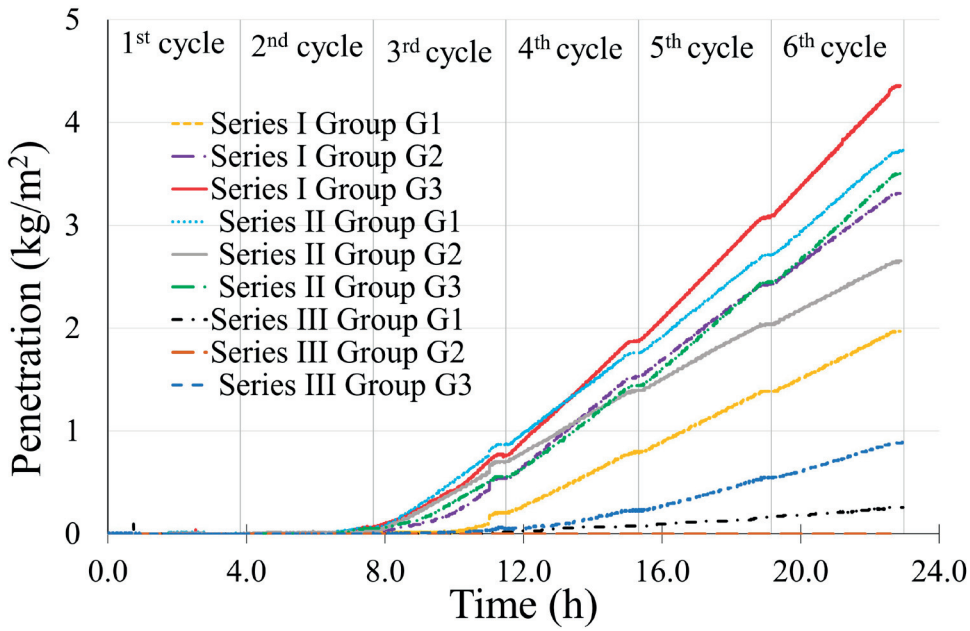

Figure 19. Average water penetration vs. time response of all Series in the second experimental campaign (B)

Table 4. Water penetration in terms of time to leakage, the amount of penetration, and leakage percentage for individual specimens of campaign B

		Specimens	Time to leakage (h)	Ave time to leakage (h)	Penetration (kg/m^2)	Ave Penetration (kg/m^2)	Leak in the 6^{th} cycle (%)	Ave (%)	Tot leak (%)	Ave (%)
Campaign B	Series I group G1	B-I-F-1	11.0	10.4	1.1	2.0	1.3	2.6	0.8	1.5
		B-I-F-2	9.9		2.2		3.0		1.7	
		B-I-F-3	10.1		2.7		3.6		2.1	
		B-I-F-4	10.4		1.9		2.6		1.4	
	Series I group G2	B-I-R-1	8.4	8.8	3.5	3.3	4.6	4.0	2.6	2.5
		B-I-R-2	6.9		2.8		3.3		2.2	
		B-I-R-3	9.4		6.3		7.8		4.8	
		B-I-R-4	10.4		0.6		0.2		0.4	
	Series I group G3	B-I-AF-1	8.5	8.2	3.5	4.4	5.3	5.8	2.7	3.3
		B-I-AF-2	9.4		5.9		8.8		4.4	
		B-I-AF-3	6.6		8.0		8.9		6.1	
		B-I-AF-4	-		0.0		0.0		0.0	
	Series II group G1	B-II-F-1	8.1	9.4	3.5	3.7	4.3	4.6	2.7	2.8
		B-II-F-2	15.0		0.5		1.3		0.4	
		B-II-F-3	6.3		4.6		5.6		3.4	
		B-II-F-4	8.0		6.3		7.1		4.8	
	Series II group G2	B-II-R-1	7.8	8.6	3.9	2.7	4.5	2.8	3.0	2.0
		B-II-R-2	8.2		2.8		2.6		2.1	
		B-II-R-3	11.0		0.3		0.2		0.2	
		B-II-R-4	7.5		3.6		3.8		2.7	
	Series II group G3	B-II-AF-1	11.1	9.0	2.6	3.5	4.3	4.8	2.0	2.7
		B-II-AF-2	6.6		3.7		3.6		2.8	
		B-II-AF-3	9.0		4.5		6.8		3.4	
		B-II-AF-4	9.1		3.3		4.5		2.5	
	Series III group G1	B-III-F-1	10.8	-	0.9	0.2	1.4	0.4	0.7	0.2
		B-III-F-2	-		0		0		0	
		B-III-F-3	-		0		0		0	
		B-III-F-4	-		0		0		0	
	Series III group G2	B-III-R-1	-	-	0	0	0	0	0	0
		B-III-R-2	-		0		0		0	
		B-III-R-3	-		0		0		0	
		B-III-R-4	-		0		0		0	
	Series III group G3	B-III-AF-1	-	-	0.0	0.9	0	1.4	0	0.7
		B-III-AF-2	10.9		1.3		2.4		1.0	
		B-III-AF-3	8.6		2.2		3.1		1.6	
		B-III-AF-4	-		0.0		0		0	

It was previously mentioned that water mainly penetrated through the brick-mortar interface, particularly from the bed joint between the first and the second course. Although no differential air pressure was applied in the second experimental campaign (B), the driving potentials forcing water to penetrate might be gravity and kinetic energy of water drops, as stated by Straube and Burnett [67].

The obtained results suggest that water penetration is highly dependent on the water content of specimens (saturation level), brick absorption properties, and the water spray rate. However, it can be seen that the effect of joint profile finish on water penetration is insignificant since the highest amount of leakage in Series I was recorded for group G3 whereas, in Series II, specimens of group G1 had the greatest amount of water penetration.

Table 4 summarizes the results of water penetration for each specimen tested in the second campaign. Also, the approximate time when water penetration started is presented in Table 4. The average time for water to start penetrating varied between 8 and 10 hours for all groups within Series I and II. All specimens in Series I and II experienced water leakage, except specimen B-I-AF-4. Interestingly, the greatest amount of water penetration, 8.0 kg/m^2, was recorded for Specimen B-I-AF-3, whereas no penetrated water was observed for specimen B-I-AF-4. For Series III, no penetration was registered, except B-III-F-1, B-III-AF-2, and B-III-AF-3. Moreover, no water penetration was observed for Series III group G2, specimens prepared with low suction bricks and raked joint profile, which might depend on the fact that the specimens were not saturated, see Figure 15.a.

It should be mentioned that the penetrated water mainly passed through the brick-mortar interface, indicating the importance of the interfacial zone on masonry's resistance to WDR. For instance, in nine out of twelve specimens in Series III, the amount of water penetration was nearly equal to 0 kg/m^2. Compared to Series I and II, the sharp contrast is attributed to continuous contact in the brick-mortar interface and the absence of known defects. However, in specimens B-III-F-1, B-III-AF-2, and B-III-AF-3, a water penetration of 0.9 kg/m^2, 1.3 kg/m^2, and 2.2 kg/m^2, respectively, were registered, indicating that the quality of the workmanship might not have been as high as the other specimens of Series III. It should be further observed that the amount of penetrated water varied within a considerable range also in Series I and II, between 0 – 8 kg/m^2 and 0.3 – 6.3 kg/m^2, respectively. Figure 20 shows the significant variability in the results of water penetration in the individual specimens of Series I group G2. Accordingly, several factors might contribute to the large scatter in the results of water penetration by comparing individual specimens even with similar brick and joint profile; a) the quality of the workmanship to completely fill the joints might differ between specimens, b) the bond, i.e., the adequate contact between brick and mortar might not be achieved in some specimens, and c) there is a large variability in the absorption properties of bricks and mortar.

The obtained results highlight the impact of water absorption properties of bricks on the leakage through specimens, as water penetration in specimens prepared with low suction bricks was considerably lower than those prepared with medium suction bricks type I and II, as already noted by Ritchie and Plewes [77]. Moreover, comparing water penetration of each group within each Series shows that the effect of mortar joint profile on water penetration is negligible.

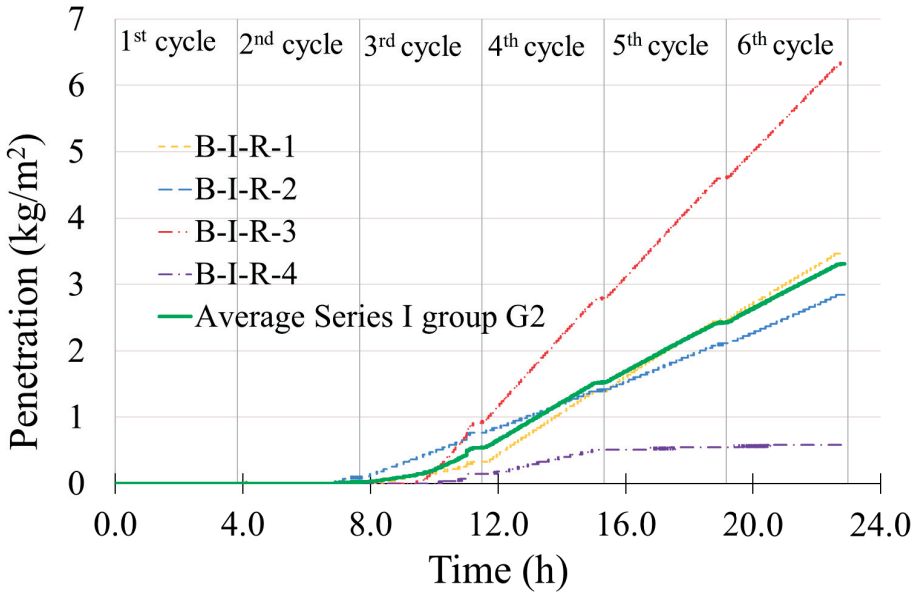

Figure 20. Water penetration in the individual specimens of Series II group G2 within campaign B

The results of total leakage and leakage during the sixth cycle are summarized in Table 4. Leakage herein is defined as the ratio between the amount of sprayed water and the amount of penetrated water. According to guidelines presented in the ASHRAE Standard 160:2009, a one percent leakage of WDR is normally assumed during heat, air, and moisture (HAM) simulations. In the light of the present results, WDR events with an intensity below 3.8 l/m^2/h might not result in significant, if any, water leakage through a clay brick masonry veneer with a thickness of 120 mm. Yet, a water spray rate of 6.3 l/m^2/h during 21 h might lead to a leakage of up to 8.9 % of the sprayed water.

The amount of leakage highly depends on the absorption properties of bricks and generally occurs once the masonry is close to saturation. It should be further noticed that leakage might happen in masonry specimens after around 8 h – 10 h of exposure to WDR with an intensity of 6.3 l/m^2/h, depending on the sorptivity and water absorption capacity of masonry. As mentioned in Section 2.1, most WDR events in Sweden take around 1 h to 4 h with an intensity of less than 1 mm/h, indicating the low probability of a WDR event with the duration of 21 h and an intensity of 6.3 l/m^2/h.

The importance of filling the head joints to control water penetration in masonry walls is noteworthy, as it is considered one of the most important factors influencing water penetration [5, 70, 71, 78]. The common workmanship techniques to fill the head joints are known as “pushing the head joint” and “buttering”, as illustrated in

Figure 21, buttering being recommended as the better one [5]. However, as mentioned in Section 3.3.3, the workmanship technique employed in this study was the so-called pushing of the head joint.

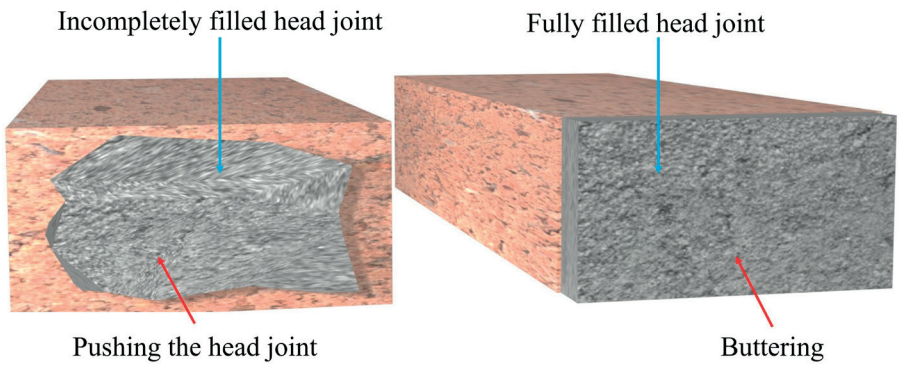

Figure 21. Common workmanship methods for filling the head joints

5 Summary of the appended papers

Paper I

Repointing is a maintenance technique with the potential of reducing the WDR-related issues of eroded mortar joints though the criteria to make a rational decision on repointing are not well established. Several criteria exist to facilitate the decision on whether repointing is needed or not, yet some proposed criteria can be questioned. A review providing the results of a state-of-the-art study concerning field and laboratory methods to assess water content and water uptake caused by WDR is presented. Using the information on water content and water uptake to rationally analyze whether repointing can improve the technical condition of clay brick façades in relation to WDR action is discussed. Accordingly, destructive and non-destructive test methods to measure moisture content and water absorption in masonry façades are reviewed. It is recommended that the visual inspection, if not conclusive, be accompanied by one of the presented test methods to assess the state of the façade, leading to a more rational decision on repointing. Further, alternative maintenance techniques which may postpone the need for costlier maintenance and reveal potential defects or problems are presented.

Paper II

Brick masonry façades are widely used because of their long-term performance and high durability, yet climate agents including WDR and freezing-thawing result in inevitable deterioration and erosion of masonry façades. The test conditions of the majority of existing standards and research studies are representative of extreme WDR events, and there is a need for a simple test setup to study the resistance of masonry to WDR. Accordingly, an experimental study was conducted to study the behavior of masonry in terms of water absorption and penetration exposed to water spraying by developing a new test setup. The appearance of damp patches and their spread on the backside of the specimens was recorded using a digital camera mounted behind the specimens. Several parameters, including the brick absorption properties and different mortar joint profiles, were considered. Triplet masonry specimens were built with three different types of brick and two different types of joint profile finishes, namely flush and raked. Raked specimens were considered representative of eroded mortar joints. The specimens were exposed to a uniform water spray rate of 1.7 – 3.8 $l/m^2/h$, simulating more realistic WDR events encountered in Sweden. The obtained results indicate that water absorption is

mainly dependent on the water absorption properties of bricks, including the water absorption coefficient and water absorption capacity. In contrast, the effect of mortar joint profile on water absorption in masonry is not considerable. The first visible damp patch on the backside of the specimens appeared close to the brick-mortar interfacial zone, indicating the lower resistance of the head joints to WDR, mainly attributed to lower compaction and difficulty of workmanship to fill in joints completely.

Paper III

An experimental campaign was designed to study water absorption and penetration in triplet masonry specimens exposed to uniform water spray. The specimens were exposed to a water spray rate of 6.3 l/m^2/h and zero differential air pressure. The presented setup was equipped with two digital scales providing the opportunity to measure water absorption and penetration continuously during 23 h of testing. The results highlight the effect of brick absorption properties on water absorption and penetration. However, the impact of joint profile on water absorption and penetration was negligible. Masonry specimens prepared with low suction bricks and low absorption capacity showed better resistance to WDR than those prepared with medium suction bricks and higher absorption capacity. Further, the first dampness appeared close to the brick-mortar interface in most specimens, indicating the brick-mortar interfacial zone as the primary path for water penetration.

6 Conclusions

The response of clay brick masonry exposed to a uniform water spray was studied by employing a newly developed test setup. Two main experimental campaigns were performed, and different parameters, including water spray rate, water absorption properties of bricks, and mortar joint profile, were considered. The specimens in this study were exposed to water spray rates varying between 1.7 and 6.3 l/m^2/h, a reduction of approximately 90% in comparison with the water application rate specified in current standards and many studies. Based on the obtained results, the following conclusions can be drawn:

- The moisture absorption response of the masonry specimens was mainly dependent on the water absorption properties of the bricks.
- Prior to the surface saturation, the water absorption in masonry specimens was highly dependent on the water spray rate and water absorption coefficient of bricks. Once the surface saturation was attained, the behavior was dependent on both the water absorption coefficient of bricks and the water absorption capacity of the bricks.
- The effect of mortar joint profile on water absorption and penetration was not considerable.
- Water penetration started when the masonry specimens were nearly close to saturation, highlighting that the gained benefit from the storage capacity of masonry could postpone the occurrence of water penetration.
- The time to the appearance of the first visible damp patch on the backside of specimens was also affected by the water spray rate and absorption properties of bricks.
- The first dampness appeared close to the brick-mortar interface in the vicinity of the head joint, indicating the lower resistance of head joints to WDR. Further, the adequate filling of the head joint might affect the location and the time to the appearance of the first visible damp patch.
- For specimens exposed to a water spray rate of around 3.5 l/m^2/h, it took nearly 16 h to get a completely wet masonry specimen (i.e., reach entire dampness on the backside of masonry). Additionally, for specimens

prepared with low water absorption properties, the backside did not reach full dampness, even after 21 h of water spraying with the rate of 6.3 l/m^2/h.

- The newly developed test setup might facilitate the verification of moisture simulations as it enables continuous water absorption and penetration measurements combined with tracing of damp areas on the backside of masonry specimens.

7 Future Research

The current work provided an insight into the resistance of clay brick masonry façades to WDR. It is widely accepted among both researchers and practitioners that differential air pressure induced by wind is the governing agent that influences water penetration in masonry. The focus of the current study was to produce low water spray rates, which are uniform and representative of WDR in Sweden, while the effect of pressure stemming from wind has so far not been considered. However, the developed test setup presented in this study is capable of producing different levels of air pressure. An important point for future research is to study masonry exposure to WDR with different levels of differential air pressure.

The masonry specimens in the present project were prepared in laboratory conditions and built without any known defects such as cracks. Based on the present as well as previous research, it is believed that the brick-mortar interface provides a path of least resistance for water penetration. Further, many of the existing masonry façades are cracked and eroded due to differential movements, reinforcement corrosion, and harsh weather conditions. These imperfections can provide other similar pathways for water to penetrate through the masonry. Thus, to better understand the effect of cracks and other imperfections, there is a need to study water absorption and penetration in such masonry specimens both in laboratory and field.

Imperfections may also be caused by workmanship, and the current work revealed the importance of workmanship in filling the joints and brick-mortar interface on the resistance of masonry to WDR. Another critical step is comparing the effect of different workmanship methods on the resistance of masonry to driving rain.

The masonry specimens in the present project were prepared with solid bricks. Yet, many clay brick masonry façades in Sweden have been constructed with perforated bricks. Thus, studying water absorption and water penetration in masonry with perforated bricks might generate useful knowledge.

In the absence of differential air pressure, the expected driving force to push water through masonry seems to be the gravitational force. In the current study, water penetration could be detected in the absence of a pressure difference. Thus, there is a need to shed light on the effect of hydrostatic pressure due to gravitational forces on leakage.

Simulations of moisture accumulation in masonry walls with other configurations than studied in the present project might be a possible way to extend the validity of the present results. This is especially interesting in the case of thick masonry walls, in which experimental studies might be much more difficult to be carried out in practice.

Simulations could further be used to analyze moisture safety in external walls with the external leaf consisting of clay brick masonry, especially in the light of the indications that gravity might be an important driving force for water penetration in walls exposed to WDR.

Techniques that are used to apply new mortar during repointing may affect water absorption and penetration into clay brick masonry. Compared to the traditional method to fill the raked joints with a trowel by hand, machine-driven equipment to apply new mortar is often used. The mortar used for machinery equipment usually has higher water content, resulting in difficulties in compacting the mortar. Consequently, filling mortar joints with machine-driven equipment may result in lower strength, air voids, and poor contact between bricks and mortar. Thus, the effects of different methods to fill the raked joints should be investigated.

Eventually, there is a need to develop a solid knowledge to make rational decisions on repointing and address the following questions:

a) The tools and methods that can be employed to rake out the mortar.

b) The depth to which the existing mortar should be raked out.

c) The compatibility of the repointing mortar with the existing units and mortar.

References

[1] M. Abuku, H. Janssen, and S. Roels, "Impact of wind-driven rain on historic brick wall buildings in a moderately cold and humid climate: Numerical analyses of mould growth risk, indoor climate and energy consumption," *Energy and Buildings,* vol. 41, no. 1, pp. 101-110, 2009/01/01/ 2009, doi: https://doi.org/10.1016/j.enbuild.2008.07.011.

[2] S. Shahreza, M. Molnár, J. Niklewski, I. Björnsson, and T. Gustavsson, "Making decision on repointing of clay brick facades on the basis of moisture content and water absorption tests results–a review of assessment methods," in *Brick and Block Masonry-From Historical to Sustainable Masonry*: CRC Press, 2020, pp. 617-623.

[3] *ASTM E514 / E514M-14a, Standard Test Method for Water Penetration and Leakage Through Masonry*, A. International, West Conshohocken, PA, 2014.

[4] R. Cacciotti, "Brick masonry response to wind driven rain," *Engineering Structures,* vol. 204, p. 110080, 2020.

[5] F. Slapø, T. Kvande, N. Bakken, M. Haugen, and J. Lohne, "Masonry's Resistance to Driving Rain: Mortar Water Content and Impregnation," *Buildings,* vol. 7, no. 3, p. 70, 2017.

[6] J. Ribar, "Water permeance of masonry: a laboratory study," in *Masonry: Materials, Properties, and Performance*: ASTM International, 1982.

[7] *NEN 2778:2015 nl. Vochtwering in gebouwen (Moisture control in buildings)*, Nederlands, 2015.

[8] *NBI 29/1983 Mørtler. Tetthet mot slagregn (Mortars. Resistance to driving rain)*, Norges byggforskningsinstitutt: Oslo, Norway, 1983.

[9] C. Groot and J. Gunneweg, "The influence of materials characteristics and workmanship on rain penetration in historic fired clay brick masonry," *Heron, 55 (2),* 2010.

[10] R. R. Vilató, "WATER PENETRATION TEST ON CONCRETE BLOCK MASONRY," in *the 15th International Brick and Block Masonry Conference*, Florianópolis – Brazil, 2012.

[11] J. C. Z. Piaia, M. Cheriaf, J. C. Rocha, and N. L. Mustelier, "Measurements of water penetration and leakage in masonry wall: Experimental results and numerical simulation," *Build. Environ.,* vol. 61, pp. 18-26, 2013.

[12] K. B. Anand, V. Vasudevan, and K. Ramamurthy, "Water permeability assessment of alternative masonry systems," *Build. Environ.,* vol. 38, no. 7, pp. 947-957, 2003/07/01/ 2003, doi: https://doi.org/10.1016/S0360-1323(03)00060-X.

[13] T. Ritchie, "Small-panel method for investigating moisture penetration of brick masonry," in "Internal Report (National Research Council of Canada. Division of Building Research); no. DBR-IR-160," National Research Council of Canada, 1958/09/01 1958.

[14] S. Van Goethem, N. Van Den Bossche, and A. Janssens, "Watertightness Assessment of Blown-in Retrofit Cavity Wall Insulation," *Energy Procedia,* vol. 78, pp. 883-888, 2015/11/01/ 2015, doi: https://doi.org/10.1016/j.egypro.2015.11.012.

[15] M. E. Driscoll and R. E. Gates, "A Comparative Review of Various Test Meteods for Evaluating the Water Penetration Resistance of Concrete Masonry Wall Units," in *Masonry: Design and Construction, Problems and Repair*: ASTM International, 1993.

[16] L. R. Baker and F. W. Heintjes, "Water leakage through masonry walls," *Architectural Science Review,* Article vol. 33, no. 1, pp. 17-23, 1990, doi: 10.1080/00038628.1990.9696662.

[17] N. Van Den Bossche, M. Lacasse, and A. Janssens, "Watertightness of masonry walls: an overview," in *12th International conference on Durability of Building Materials and Components (XII DBMC-2011)*, 2011, vol. 1: FEUP Edições, pp. 49-56.

[18] S. Kahangi Shahreza, J. Niklewski, and M. Molnár, "Experimental investigation of water absorption and penetration in clay brick masonry under simulated uniform water spray exposure," *Journal of Building Engineering,* vol. 43, p. 102583, 2021/11/01/ 2021, doi: https://doi.org/10.1016/j.jobe.2021.102583.

[19] R. Forghani, Y. Totoev, S. Kanjanabootra, and A. Davison, "Experimental investigation of water penetration through semi-interlocking masonry walls," *Journal of Architectural Engineering,* vol. 23, no. 1, p. 04016017, 2017.

[20] M. Lacasse, T. O'Connor, S. Nunes, and P. Beaulieu, "Report from Task 6 of MEWS project: Experimental assessment of water penetration and entry into wood-frame wall specimens-final report," *Institute for Research in Construction, RR-133, Feb,* 2003.

[21] A. Rathbone, *Rain and air penetration performance of concrete blockwork*. Cement and Concrete Association, 1982.

[22] H. Hens, S. Roels, and W. Desadeleer, "Rain leakage through veneer walls, built with concrete blocks," in *CIB W40 meeting in Glasgow*, 2004.

[23] A. Fried, A. Tovey, and J. Roberts, *Concrete masonry designer's handbook*. CRC Press, 2014.

[24] S. M. Tindall, "Repointing Masonry—Why Repoint?," *Old-House Journal,* pp. 24-31, January/February 1987.

[25] B. Brief, "Maintenance of Brick Masonry," *Brick Industry Association, Technical Notes on Brick Construction,* vol. 46, pp. 1-11, December 2017.

[26] J. G. Stockbridge, "Repointing masonry walls," *APT bulletin,* vol. 21, no. 1, pp. 10-12, 1989.

[27] S. Johnson, "The neglected craft of repointing–an architect's view," ed: Crown copyright NSW Heritage Office & the author, 2000.

[28] P. Maurenbrecher and J. E. Lindqvist, "RILEM TC 203-RHM: Repair mortars for historic masonry : Requirements for repointing mortars for historic masonry," (in eng), *Materials and Structures,* article vol. 45, no. 9, pp. 1303-1309, 2012 2012. [Online]. Available: http://urn.kb.se/resolve?urn=urn:nbn:se:ri:diva-2706.

[29] A. H. P. Maurenbrecher, K. Trischuk, M. Z. Rousseau, and M. I. Subercaseaux, "Repointing mortars for older masonry buildings: design considerations," (in eng), *Construction Technology Update; no. 67,* 2008/03/01 2008, Art no. 6 p., doi: 10.4224/21274782.

[30] P. M. C. L. Paul Jeffs, "Repointing Masonry Walls – Matching the Techniques for Success or Failure," ed. Technical Workshop Restoration, Reconstruction and Maintenance of Masonry Structures, Dalhousie University Continuing Technical Education: Conservation of Heritage Structures & Older Buildings.

[31] R. Veiga and F. Carvalho, "Some performance characteristics of lime mortars for rendering and repointing ancient buildings," in *Proc. Br. Masonry Soc. No. 8*, 1998, pp. 353-356.

[32] D. Young, "Repointing mortar joints: some important points," in *Australia ICOMOS Conference*, Adelaide Australia, 5-8 November 2015.

[33] C. W. Westermann, Heinrich and Schulz, Jens-Uwe, "Increased Durability of Repointing In Historical Masonry – Engineering Model and Sensitivity Analysis," presented at the 13th Canadian Masonry Symposium, Halifax, Canada, 4-7 June, 2017.

[34] A. Maurenbrecher, K. Trischuk, M. Rousseau, and M. Subercaseaux, "Key Considerations for Repointing Mortars for the Conservation of Older Masonry (IRC-RR-225)," *Canada: Institute for Research in Construction, National Research Council of Canada, Ottawa,* 2007.

[35] I. M. Griffin, "Deterioration mechanisms of historic cement renders and concrete," Doctoral dissertation, University of Edinburgh, 2013.

[36] M. Holland, *Practical Guide to Diagnosing Structural Movement in Buildings*. John Wiley & Sons, 2012.

[37] B. Brief, "Repointing (Tuckpointing) Brick Masonry," *Brick Industry Association,* July 2005.

[38] K. Wang, D. C. Jansen, S. P. Shah, and A. F. Karr, "Permeability study of cracked concrete," *Cement and concrete research,* vol. 27, no. 3, pp. 381-393, 1997.

[39] C.-M. Aldea, S. P. Shah, and A. Karr, "Permeability of cracked concrete," *Materials and structures,* vol. 32, no. 5, pp. 370-376, 1999.

[40] B. Blocken and J. Carmeliet, "A review of wind-driven rain research in building science," *Journal of Wind Engineering and Industrial Aerodynamics,* vol. 92, no. 13, pp. 1079-1130, 2004/11/01/ 2004, doi: https://doi.org/10.1016/j.jweia.2004.06.003.

[41] E. Cho, C. Yoo, M. Kang, S.-u. Song, and S. Kim, "Experiment of wind-driven-rain measurement on building walls and its in-situ validation," *Build. Environ.,* vol. 185, p. 107269, 2020/11/01/ 2020, doi: https://doi.org/10.1016/j.buildenv.2020.107269.

[42] B. Blocken, D. Derome, and J. Carmeliet, "Rainwater runoff from building facades: A review," *Build. Environ.,* vol. 60, pp. 339-361, 2013/02/01/ 2013, doi: https://doi.org/10.1016/j.buildenv.2012.10.008.

[43] A. Erkal, D. D'Ayala, and L. Sequeira, "Assessment of wind-driven rain impact, related surface erosion and surface strength reduction of historic building materials," *Build. Environ.,* vol. 57, pp. 336-348, 2012.

[44] M. Abuku, H. Janssen, J. Poesen, and S. Roels, "Impact, absorption and evaporation of raindrops on building facades," *Build. Environ.,* vol. 44, no. 1, pp. 113-124, 2009/01/01/ 2009, doi: https://doi.org/10.1016/j.buildenv.2008.02.001.

[45] J. Carmeliet and B. Blocken, "Driving rain, rain absorption and rainwater runoff for evaluating water leakage risks in building envelopes," in *9th International Conference on Performance of Exterior Envelopes of Whole Buildings (Buildings IX)*, 2004.

[46] G. Robinson and M. C. Baker, "Wind-driven rain and buildings," in "Technical Paper (National Research Council of Canada. Division of Building Research); no. DBR-TP-445," National Research Council of Canada, 1975/07 1975.

[47] A. J. Newman, D. Whiteside, and P. B. Kloss, "Full-scale water penetration tests on twelve cavity fills—Part II. Three built-in fills," *Build. Environ.,* vol. 17, no. 3, pp. 193-207, 1982/01/01/ 1982, doi: https://doi.org/10.1016/0360-1323(82)90039-7.

[48] V. Korsgaard and T. L. Madsen, *CORRELATION BETWEEN MEASURED DRIVING RAIN AND COMPUTED DRIVING RAIN*. TECHN. UNIV. DENMARK, HEAT INSULATION LABOR., 1962.

[49] R. E. Lacy, "Driving rain maps and the onslaught of rain on buildings," in *Proc. of CIB/RILEM Symposium on Moisture Problems in Buildings, Helsinki, 1965*, 1965.

[50] A. Best, "The size distribution of raindrops," *Quarterly Journal of the Royal Meteorological Society,* vol. 76, no. 327, pp. 16-36, 1950.

[51] J. Straube and E. Burnett, "Simplified prediction of driving rain on buildings," in *Proceedings of the international building physics conference*, 2000: Eindhoven University of Technology Eindhoven, the Netherlands, pp. 375-382.

[52] *EN ISO 15927-3, Hygrothermal performance of buildings-Calculation and presentation of climatic data. Part 3: calculation of a driving rain index for vertical surfaces from hourly wind and rain data*, 2009.

[53] E. Choi, "Determination of wind-driven-rain intensity on building faces," *Journal of Wind Engineering and Industrial Aerodynamics,* vol. 51, no. 1, pp. 55-69, 1994.

[54] B. Blocken and J. Carmeliet, "Overview of three state-of-the-art wind-driven rain assessment models and comparison based on model theory," *Build. Environ.,* vol. 45, no. 3, pp. 691-703, 2010/03/01/ 2010, doi: https://doi.org/10.1016/j.buildenv.2009.08.007.

[55] B. S. Institution, *Code of Practice for Assessing Exposure of Walls to Wind-driven Rain*. British Standards Institution, 1992.

[56] "https://www.smhi.se/data." SMHI, "SMHI Öppna data". (accessed September 2020).

[57] C. Hall and W. D. Hoff, *Water transport in brick, stone and concrete*, 2nd Edition ed. CRC Press, 2011.

[58] Z. Liu, P. Zhang, J. Bao, and Y. Hu, "Numerical Simulation of Water Transport in Unsaturated Recycled Aggregate Concrete," (in English), *Frontiers in Materials,*

Original Research vol. 7, no. 314, 2020-September-21 2020, doi: 10.3389/fmats.2020.560621.

[59] M. Karoglou, A. Moropoulou, Z. Maroulis, and M. Krokida, "Water sorption isotherms of some building materials," *Drying technology,* vol. 23, no. 1-2, pp. 289-303, 2005.

[60] H. M. Künzel, "Simultaneous heat and moisture transport in building components," *One-and two-dimensional calculation using simple parameters. IRB-Verlag Stuttgart,* vol. 65, 1995.

[61] L. Mengel, H.-W. Krauss, and D. Lowke, "Water transport through cracks in plain and reinforced concrete–Influencing factors and open questions," *Construction and Building Materials,* vol. 254, p. 118990, 2020.

[62] P. K. Mehta and P. J. Monteiro, *Concrete: microstructure, properties, and materials*. McGraw-Hill Education, 2014.

[63] P. A. Claisse, *Transport properties of concrete: Measurements and applications*. Elsevier, 2014.

[64] Ø. Birkeland and S. Svendsen, "Norwegian test methods for rain penetration through masonry walls," in *Symposium on Masonry Testing*, 1963: ASTM International.

[65] C. T. Grimm, "Masonry cracks: a review of the literature," *Masonry: materials, design, construction, and maintenance,* 1988.

[66] J. F. Straube and E. F. Burnett, "Driving rain and masonry veneer," in Water leakage through building facades: ASTM International, 1998.

[67] J. Straube and E. Burnett, "Rain control and screened wall systems," in Proc. 7th Conf. on Building Science and Technology. Durability of Buildings. Design, Maintenance, Codes and Practices. Toronto, 1997, pp. 20-21.

[68] J. F. Straube, "The Performance of Wall Systems Screened with Brick Veneer," University of Waterloo, 1994.

[69] C. L. Galitz and A. R. Whitlock, "The application of local weather data to the simulation of wind-driven rain," in Water Leakage Through Building Facades: ASTM International, 1998.

[70] C. T. Grimm, "Water permeance of masonry walls: a review of the literature," in Masonry: Materials, Properties, and Performance: ASTM International, 1982.

[71] C. C. Fishburn, D. Watstein, and D. E. Parsons, Water permeability of masonry walls. US Department of Commerce, National Bureau of Standards, 1938.

[72] S. Cornick and M. Lacasse, "An Investigation of Climate Loads on Building Façades for Selected Locations in the United States," Journal of ASTM International, vol. 6, no. 2, pp. 1-22, 2009.

[73] K. Sandin, "Fukttillstånd i autoklaverade lättbetongväggar : fältmätning av slagregnets och ytskiktets inverkan (Rapport TVBM; Vol. 3026)," Avd Byggnadsmaterial, Lunds tekniska högskola, 1987.

[74] ASTM C67 / C67M-20, Standard Test Methods for *Sampling and Testing Brick and Structural Clay Tile*, A. International, West Conshohocken, PA, 2020.

[75] *ASTM C1403 - 15, Standard Test Method for Rate of Water Absorption of Masonry Mortars*, A. International, West Conshohocken, PA, 2015.

[76] T. Ritchie and J. I. Davison, "Factors affecting bond strength and resistance to moisture penetration of brick masonry," (in eng), *ASTM Special Technical Publication,* no. 320, pp. 16-30, 1963/07/01 1963.

[77] T. Ritchie and W. G. Plewes, "A review of literature on rain penetration of unit masonry," (in eng), *Technical Paper (National Research Council of Canada. Division of Building Research),* 1957/05 1957, Art no. iii, 72 p., doi: 10.4224/40001176.

[78] C. C. Fishburn, *Water permeability of walls built of masonry units*. US Department of Commerce, National Bureau of Standards, 1942.

Printed by Media-Tryck, Lund 2019 NORDIC SWAN ECOLABEL 3041 0903

LUND UNIVERSITY

Lund University
Faculty of Engineering
Division of Structural Engineering
Report: TVBK-1055
ISBN: 978-91-87993-20-6
ISSN: 0349-4969
ISRN: LUTVDG/TVBK-21/1055 (63)

9 789187 993206